The impact of climate controlled frequency variations in sediment supply on basin margin architecture

J.F. Bijkerk

Master thesis

The impact of climate controlled frequency variations in sediment supply on basin margin architecture

J.F. Bijkerk – 0423718

October 2009

Supervisor: Dr. George Postma

Essentially, all models are wrong, but some are useful.

- George Edward Pelham Box
Empirical Model-Building and Response Surfaces (2007), 414.

Abstract

In the general sequence stratigraphic model, variations in icehouse delta architecture are solely influenced by variations in accommodation space which is dominantly controlled by eustatic variations. However, there is an ongoing debate on the importance of climate variations. These climate variations might control discharge changes and therefore sediment flux variations towards a delta, adding another potentially important control on delta architecture. To create a better understanding on the effects of climate, six analogue flume models with different discharge scenarios are generated. These are subsequently analysed by roll-over point migration-, parasequence- and system tract-analyses to examine the importance of the discharge component in delta architecture. For these analyses video imaging, 3D digital height models and lacquer peels are used.

In this thesis, specifically the effects of discharge frequency variations on icehouse delta architecture are examined. The effects of discharge are quantified with a newly developed representation of roll-over point migration. Significant discharge frequency related offsets from eustatically forced roll-over point migration patterns are observed. These offsets can be explained by a discharge frequency variation control on the sediment flux that works in two separate ways; 1) by directly increasing or decreasing stream power via discharge variations, therefore in- or decreasing sediment carrying capacity, resulting in a correlation with the discharge curve; 2) by rapidly altering the equilibrium slope during high frequency discharge variations, therefore increasing or decreasing stream power and sediment carrying capacity, resulting in a correlation to the discharge gradient curve. The latter control is only significant when the discharge induced disequilibrium is dominant over eustatically induced disequilibria. This situation is observed during periods of extreme frequency and amplitude variations in discharge.

The addition of a climate component would moderately increase the predictive power of the sequence stratigraphic model. However, including this parameter poses a major challenge because of its complexity. The experimental results predominantly confirm the general opinion that the rate of eustatic change provides the dominant control on delta architecture. Therefore the Exxon sequence stratigraphic model does not need modification to incorporate the effects of discharge frequency variations on the sediment flux.

Contents

1 Introduction

The internal structure of deltas is determined by the interplay between the creation of accommodation space and the sediment flux that fills this accommodation space (e.g. Muto and Steel, 1997). This concept is initially described by the sequence stratigraphic model developed by the Exxon research group (Vail et al., 1977; Jervey, 1988; Posamentier et al., 1988; Posamentier and Vail, 1988). This model predicts the internal structure of deltas based solely on variations in accommodation space. Sediment flux is considered as relatively unimportant because it is assumed that it only affects the amount of deposition and not the internal structure, although it is admitted that for occasional basins, sediment flux can be a dominant control on delta architecture (Posamentier and Allen, 1993). However, this assumption is debated. For example Schlager (1993) states that sediment flux variations play a major role via environmental or climate change. Therefore, the validity of the Exxon sequence stratigraphic model must be examined. Multiple sediment flux scenarios can be envisioned to test whether the Exxon sequence stratigraphic model must be adapted to include the sediment flux, next to variations in accommodation space.

Variations in accommodation space in (passive margin) delta settings are caused by sea level fluctuations. These fluctuations are traditionally subdivided into multiple orders, dependent on their duration. First and second order sea level fluctuations (10^7 - 10^8 yr) are generally ascribed to tectonic and tectono-eustatic movements. Third order sea level fluctuations (10^6 yr) are created by regional tectonics (e.g. Woodruff and Savin, 1989) and/or long period glacio-eustatic changes (e.g. Abels et al., 2005). Fourth to sixth order sea level variations (10^5 – 10^4 yr) are related to short period astronomical forcing, also known as Milankovitch forcing. Eccentricity (fourth order at ~100 kyr) and obliquity (fifth order at ~41 kyr) determine astronomically forced insolation changes that control the ice volume in the earth's polar regions via cyclic climate changes during icehouse periods (Hays et al., 1976; Imbrie and Imbrie, 1980). This results in high frequency and large amplitude sea level fluctuations providing a dominant control on delta architecture (Vail et al., 1977). Orbital precession (sixth order at ~22 kyr) causes cyclic climate changes at low to mid latitude and thus has little effect on sea level fluctuations, since these are forced at high Northern Hemisphere latitude (Ruddiman, 2001). However, precession significantly affects global climate, for example by determining the monsoonal intensity of Northern Africa (e.g. Rossignol-Strick et al., 1983; Tuenter et al., 2003; Meijer and Tuenter, 2007) and Asia (Clemens et al., 1996; Rahaman et al., 2009).

The sediment flux to a delta setting is dependent on numerous factors, such as lithology, relief and transfer system length (e.g. van der Zwan, 2002). However, the short term variations in sediment flux, equivalent to fourth to sixth order sea level fluctuations, are mainly dependent on climate variation and associated variations in the discharge regime (Leeder et al., 1998; van der Zwan, 2002). These climate variations are dominated by eccentricity, obliquity and precession as well. Therefore,

runoff and potentially sediment flux variations are dominantly controlled by Milankovitch forcing and vary at similar timescales as the sea level. It is therefore possible to (partially) ascribe the internal delta architecture to sediment flux variations aside from sea level variations (Schlager, 1993). The expression of sediment flux variations might be masked by, or ascribed to the dominant effect of sea level fluctuations operating on equal timescales in previous research.

Whether the sequence stratigraphic model needs updating is thus determined by the importance of this sediment flux component. This cannot be solved by studying real world deltaic systems alone. For example, in Schlager (1993) the influence of a sediment flux component is recognised in third to sixth order cycles. Contrastingly, Castelltort and Van den Driessche (2003) state that fourth to sixth order variation in sediment flux to the delta setting is buffered by the transfer subsystem. Analogue modelling in a flume tank will provide a better understanding of sequence stratigraphy because deltaic evolution and the resulting deltas can be examined in high detail with known input parameters (river discharge, sediment input, subsidence, sea level) which is impossible in real world deltaic systems.

The PHASE project is a set of six analogue modelling experiments executed by Utrecht University. Four experiments, providing end member scenarios for discharge are previously carried out. These are the In Phase (IP), the Out of Phase (OP), the High Frequency Supply Variation (HS) and the Constant Supply (CS) models. Two additional analogue models are generated for this thesis. These are the quarter phase lag of sea level on discharge (NL) and the quarter phase lag of discharge on sea level (PL). The Constant Supply model can be regarded as an equivalent of the Exxon sequence stratigraphic model.

In this thesis, the CS, IP and HS models will be examined with emphasis on the influence of the period of sediment flux cyclicity on the delta architecture during icehouse conditions. The results and their implications for the Exxon sequence stratigraphic concept will be discussed. The IP and OP models have been described and discussed extensively (Gademan, 2008). A companion paper (de Vries, 2009) treats the CS, NL and PL models to create a complete dataset.
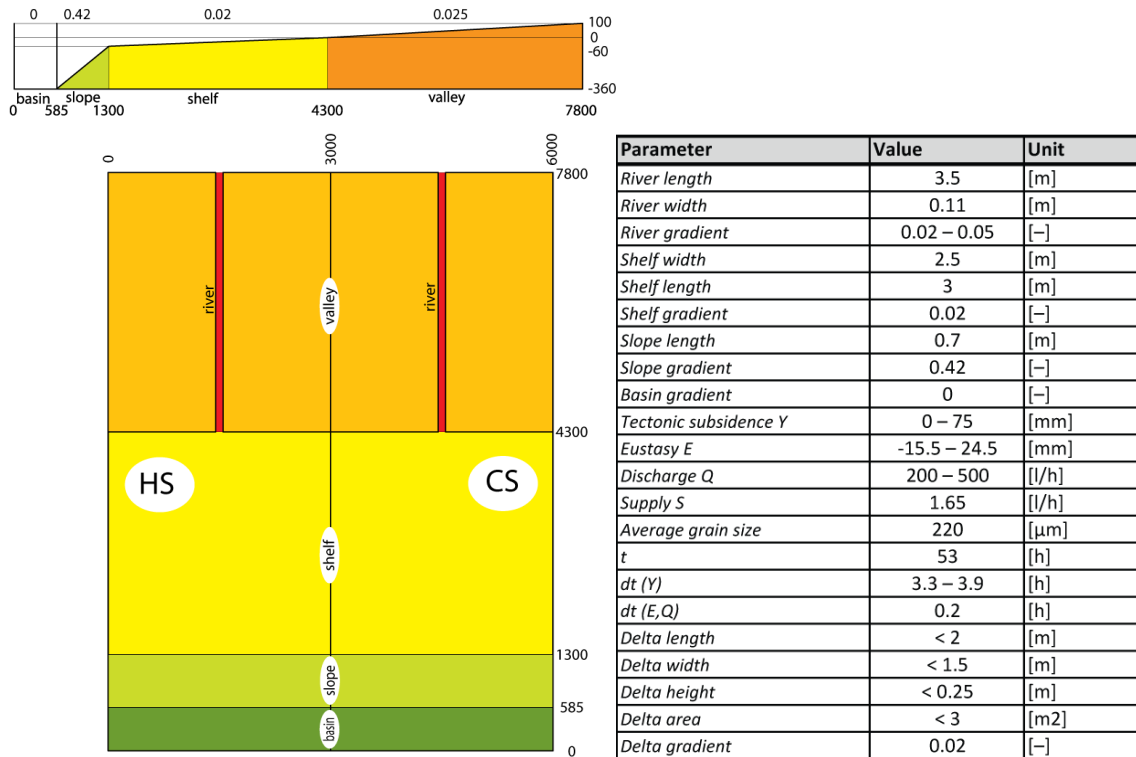
2 Methods

The PHASE project is executed at the 'Eurotank Laboratories' flume tank facility at Utrecht University. In three twin-experiments, CS & HS, IP & OP and NL & PL, the river-delta systems are modelled to examine sediment flux end-member scenarios during ice house conditions.

2.1 Experiment setup and parameters

Two equal experiment setups are constructed next to each other (Figure 1). Both contain a river valley and a shelf system on which the deltas will be modelled. Water discharge (Q) and sediment input are applied at the top of the river valley. Tectonic subsidence (Y) and sediment input (S_{in}) are at constant and equal rates during all experiments. All six models have equal scenarios for subsidence, sediment input and sea level or eustacy (E). Discharge (Q) is varied individually for each experiment.

The experiment parameters are scaled to prevent the delta from exceeding the shelf edge. The geometry of the delta will therefore remain relatively simple, resulting in lacquer peels that can be well analysed. The experiment parameters (Table 1) are primarily based on previous work (van Heijst and Postma, 2001; Meijer, 2002; van den Berg van Saparoea and Postma, 2008).

Parameter	Value	Unit
River length	3.5	[m]
River width	0.11	[m]
River gradient	0.02 – 0.05	[–]
Shelf width	2.5	[m]
Shelf length	3	[m]
Shelf gradient	0.02	[–]
Slope length	0.7	[m]
Slope gradient	0.42	[–]
Basin gradient	0	[–]
Tectonic subsidence Y	0 – 75	[mm]
Eustasy E	-15.5 – 24.5	[mm]
Discharge Q	200 – 500	[l/h]
Supply S	1.65	[l/h]
Average grain size	220	[μm]
t	53	[h]
dt (Y)	3.3 – 3.9	[h]
dt (E,Q)	0.2	[h]
Delta length	< 2	[m]
Delta width	< 1.5	[m]
Delta height	< 0.25	[m]
Delta area	< 3	[m2]
Delta gradient	0.02	[–]

←**Figure 1: Experiment setup. Deltas form on the shelf.**
→**Table 1: List of values and units of experiment parameters.**

2.2 Controls on experiment parameters

The experiment contains four variable input parameters. These are subsidence (Y), eustacy (E), sediment input (S) and discharge (Q). Sediment input and the discharge are the main controls on the *sediment flux* in the models

Sediment flux

The sediment flux to a delta is influenced by the entire sedimentary system containing a source, transport and deltaic subsystem (Figure 2) (Castelltort and Van den Driessche, 2003). Processes in the first two subsystems partially control the properties of the latter one.

Sediments are mainly generated in the source region by weathering and erosion. Climate variations are a dominant control on these processes and determine chemical and mechanical weathering rates. Climate variations also influence the amount and nature of vegetation cover, which is of major importance for weathering and erosion (Schumm and Lichty 1965; Kirkby et al, 1994; Leeder et al, 1998). Furthermore, climate determines the annual distribution of precipitation. Another important factor is the geography of a sedimentary system which includes factors such as relief, lithology, size, and temporal storage capacity (Leeder et al, 1998; Van der Zwan, 2001). Climate dependent factors as vegetation and precipitation are also of major importance for sediment transport. The transport subsystem responds in a different way than the source region. A precipitation increase leads to an increase in weathering and erosion in the long term (Kirkby et al., 1994; Nesbitt et al., 1997), but results in a rapid increase of sediment carrying capacity in the transport system (Paola et al., 1992). The increase of the sediment carrying capacity will enhance erosion in the river valley and will result in a rapid increase of the sediment flux to the delta system.

In the PHASE project, the focus is placed on short term variations. Therefore, the sediment input is set at a constant rate of 1.65 l/h per model. Variations in the deltas will be related to variations in sediment flux induced by discharge variation (200 - 500 l/h, discharge is controlled with a 10 l/h accuracy). From data derived from real word deltaic systems, the expectancy arises that a decrease in discharge will cause an increase in the river gradient, resulting in overall sedimentation in the river valley. This will thus result in a decrease in the sediment flux to the delta. An increase in discharge will result in erosion in the valley, and in a higher sediment flux to the delta (Van den Berg van Saparoea and Postma, 2008).
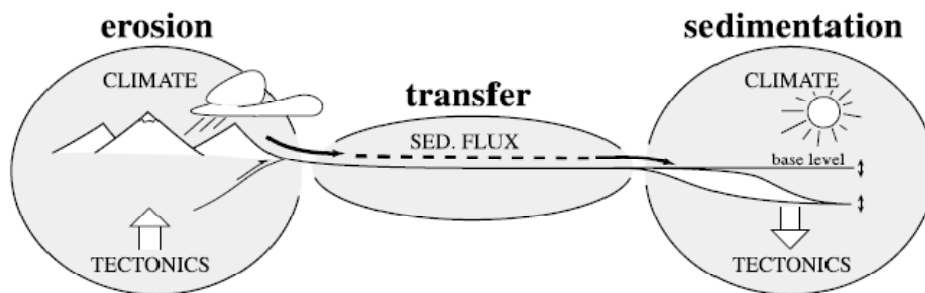
Figure 2: Schematic representation of a sediment flux system and the subdivision into different systems Adapted from: (Castelltort and Van den Driessche, 2003).

<u>Subsidence</u>

Subsidence is applied to create sufficient accommodation space to limit erosion and preserve strata in the lacquer peels of the models. Furthermore, progradation beyond the shelf margin is prevented in this manner. The subsidence is focussed in a broad channel at the distal shelf to slightly guide the depositional area, so each delta model forms in a similar shape. Subsidence is applied by manually lowering spindles below the experiment setup (Figure 5).
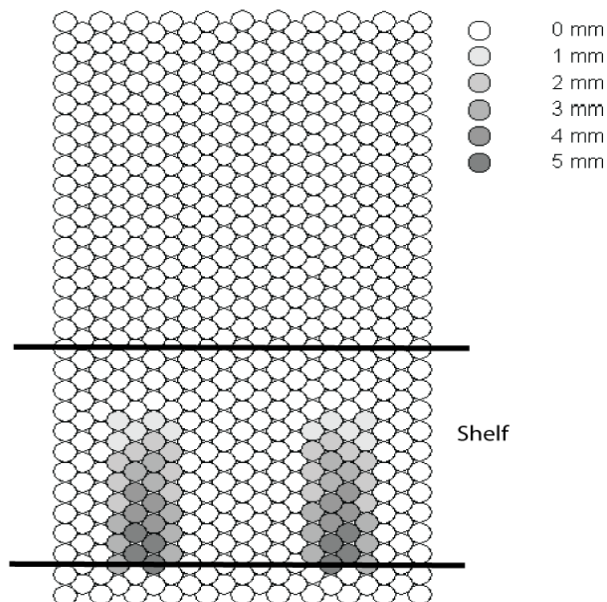

Figure 3: Schematic overview of the applied subsidence per time step. Each circle represents an adjustable spindle. Subsidence is applied in the distal shelf and on the shelf edge. Main accommodation space is thus created near the shelf edge.

<u>Eustacy</u>

Eustacy is controlled using a manually adjustable overflow near the tank edge with a precision of 0.1 mm.

2.3 Discharge scenarios

<u>Constant Discharge & High Frequency Discharge Variation</u>

The constant discharge experiment (CS) mimics the Exxon sequence stratigraphic model. River discharge and thus sediment carrying capacity do not vary in this experiment resulting in a constant sediment flux to the delta. The high frequency discharge variation (HS) represents a system where the frequency of discharge variation is three times higher than that of the sea level variation. Such a system can be easily envisioned in recent geologic history. Sea level corresponds to eccentricity dominated cyclicity (~100 kyr) while climate change at most latitudes corresponds to obliquity (~41 kyr) or precession (~23 kyr) forcing. The experiment was carried out by D. Mikes in 2008.

In Phase & Out of Phase Discharge Variation

The in & out of phase discharge variation scenarios (IP & OP) are examined in Gademan (2008) and are based on the theory proposed by Leeder et al. (1998), suggesting different sediment yield scenarios as a response to climate change. These scenarios represent two direct and opposite climate responses on insolation variation. The in-phase scenario (IP) combines high sea level with high discharge. The out of phase scenario (OP) assumes the inverse relationship, i.e., high sea level is combined with low discharge. This experiment was carried out by S. Hahn and M. Van Dijk in 2007.

Negative & Positive Phase Lag Discharge Variation

The quarter phase lag of sea level on discharge (NL) reflects the expected relation between sea level and discharge, both acting on the same astronomical forcing mechanism. The NL scenario is explained by the (almost) direct response of climate to insolation variations, resulting in a direct response of the sediment flux, while the sea level variation lags insolation forcing. The maximum ice volume and thus lowest sea level is not obtained at the lowest insolation value but at the point where accumulation and ablation of ice volume are equal. This inflection point is a quarter phase later than the minimum insolation value. The quarter phase lag of discharge of sea level scenario (PL) reflects a situation that might occur on the southern hemisphere on precession timescale when sea level forcing is located on the northern hemisphere. This experiment was carried out by J. de Vries and J.F. Bijkerk in 2008.
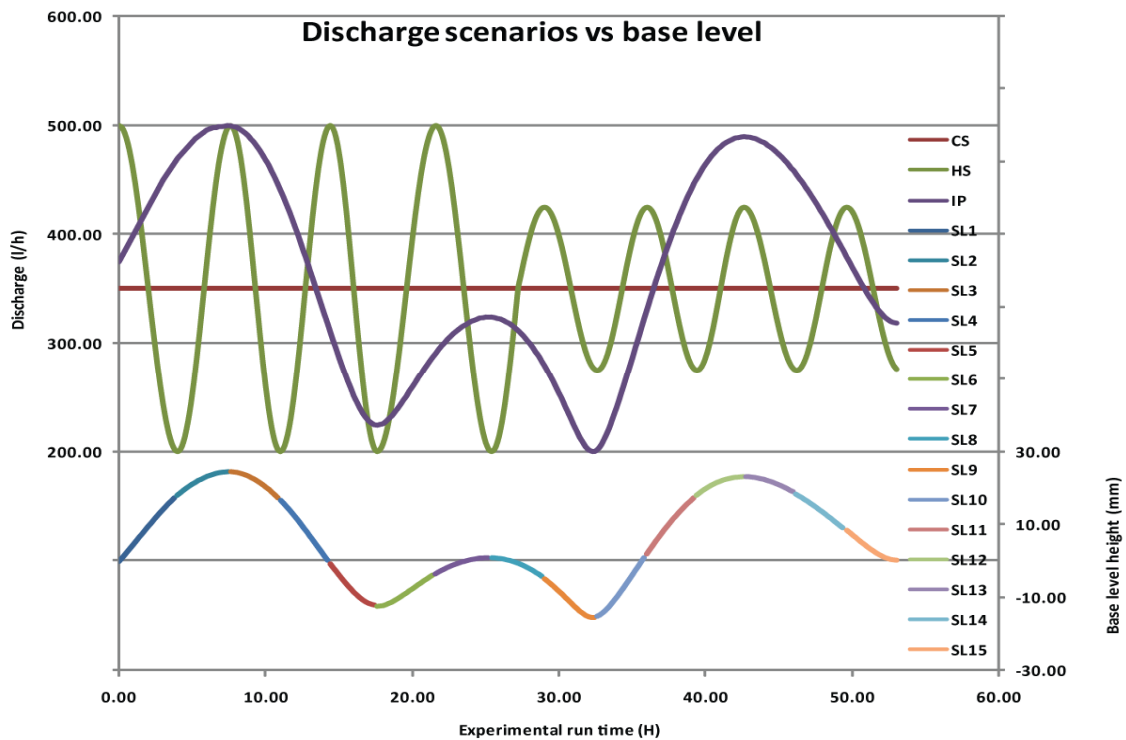

Figure 4: Discharge curves for CS, HS and IP scenarios. Sea level curve is subdivided into the 15 experiment runs.

2.4 Experiment run

The entire experiment is subdivided in 15 time steps of about 3.5 h of experiment run time.
Each step consists of the following steps.

- Set sea level by filling the tank to the overflow level

- Experiment run, water flowing to delta

- Lowering of sea level

- Laser valley height modelling

- Optional "reference height model measurement"

- Photo height modelling.

- Applying of subsidence

- Sea level up and down in order to let sand sag

- Laser valley height modelling after applying subsidence

- Photo height model run after applying subsidence

A tracer material is used at sea level maxima and minima to provide time constraints in the lacquer peels of the deltas. Between experiment runs the sand colour is changed for clearer interpretation of the lacquer profiles and video images. Discharge and sea level are manually adjusted every 12 minutes during each experiment run.

2.5 Data retrieval

Digital elevation models (DEMs), lacquer peels and video images are made of every delta.

Digital elevation models

The deltas are surveyed using a photogrammetry robot system. This system allows for high resolution scans (100 micron) of the changing delta exterior architecture in between experiment runs. From the survey, Digital Elevation Models (DEMs) are created using the SANDPHOX program. The program interlays all individual components of the survey and accurately transforms the data into an x,y,z coordinate system. This results in a typical resolution of 500.000 points for each of the deltas. The accuracy of the photogrammetry of the system is higher than 25 µm (horizontal) and 100 µm (vertical). The models are processed using the commercially available SURFER and PETREL geological software.

Lacquer peels

For interpretation of the internal delta architecture, six lacquer peel sections are selected for each of the models. These sections provide two centre (3 & 4), two side (2 & 5) and two condensed sequence

sections (1 & 6). The positions of all the profiles are indicated in Figure 5. Emphasis is placed on the centre profiles, because these provide the best overview of the differences between the experiments due to the lack of erosion. Both parasequence and systems tract interpretations are superimposed on lacquer peel images. The sections are divided into timelines that are preserved due to the tracer material. The lacquer peels are also compared from time-lapse video-images of the experiment to examine the timing of formation of different surfaces, e.g. Erosional Unconformities (EUs) and Maximum Flooding Surfaces (MFSs).
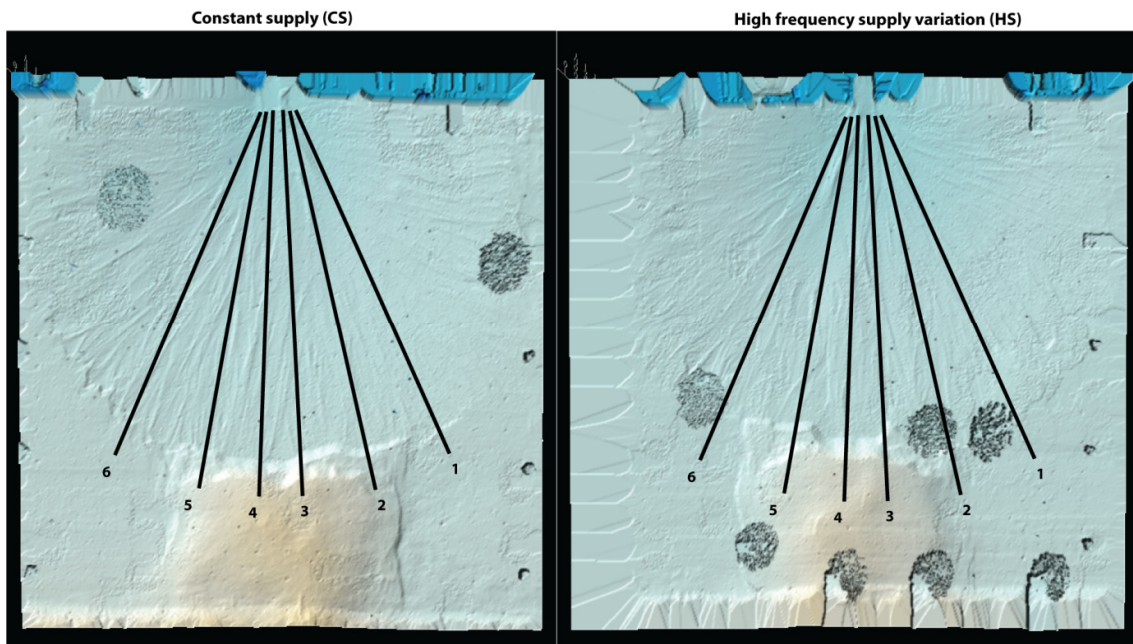

Figure 5: Overview of lacquer peel positions. Height models are created using the program Surfer. Blue areas indicate high areas (delta). Orange indicates the area influenced by the subsidence. All of the lacquer peels are numbered, sections 1 & 6 are condensed sequence profiles, 2 & 5 are side profiles and 3 & 4 are centre profiles.

Video images

Video images are created during the experiment by two 20 second time-lapse cameras and stored on a local hard drive. Afterwards a movie is created with VideoMach software.

3 Experiment results

The entire results of the CS and HS models can be found in appendix 1 (DVD). In this appendix, time-lapse video images of the experiments, lacquer peel section photos, the DEMs in xyz-coordinates and as SURFER grid file and the experiment logbook. The observations during the experiment runs are summarized in Tables 2 and 3.

Constant Supply (CS)			
Time	**SL**	**Q**	**Event**
T0-T1	Rising	Constant	Sedimentation of sheetflows on entire delta.
	Rising	Constant	Slowly retrograding sheetflows.
T1-T2	Rising	Constant	Back-stepping of delta, continued depostion of sheetflows.
	Highstand	Constant	Delta continues sheet deposition near previous back-step.
T2-T3	Highstand	Constant	Delta slowly starts prograding from previous back step onwards, deposition concentrated in broad channels at centre and right side of delta (seen from delta front)
	Falling	Constant	Sheet flow on top of delta, channel flow frequently shifting paths at delta front, occasionally toe sets forming.
T3-T4	Falling	Constant	More stationary channel flow forming small lobes at delta front.
	Falling	Constant	Flow concentrated at centre of the delta, forming larger lobes. Rapid progradation.
T4-T5	Falling	Constant	Flow still concentrated near delta. Occasional break through of narrow high velocity off-centre channels, resulting in occasional rapid progradation.
	Lowstand	Constant	Rapid progradation at centre of delta front, other parts of delta mainly exposed.
T5-T6	Lowstand	Constant	Progradation continues mainly at centre of delta front, other parts of delta mainly exposed.
	Rising	Constant	Progradation slows down, aggradation at end of time step.
T6-T7	Rising	Constant	Back-step, sedimentation over large parts of delta except left part of delta.
	Highstand	Constant	Aggradation via broad channels on large parts of delta.
T7-T8	Highstand	Constant	At first aggradation, later on mainly progradation via frequently shifting channels on large parts of delta except the left.
	Falling	Constant	Progradation in channels on large parts of delta, channels become more stationary.
T8-T9	Falling	Constant	Rapid progradation in channels mainly through the centre of the delta front.
	Lowstand	Constant	Progradation spreading towards the sides of the delta front as well.
T9-T10	Lowstand	Constant	Aggradation, mainly in tectonically influenced area. Other parts of the delta exposed.
	Rising	Constant	Aggradation, mainly in tectonically influenced area. Later on slowly retrograding.
T10-T11	Rising	Constant	Backstepping, sheetflows in large parts of the delta.
	Rising	Constant	Backstepping, sheetflows in almost entire delta.
T11-T12	Rising	Constant	Second back-step, small active area of delta. Sheetflows
	Highstand	Constant	Sheetflows in active area of delta.
T12-T13	Highstand	Constant	Aggradation at position of last back-step.
	Falling	Constant	Little progradation over position of last back-step. Mainly deposition in centre and right side of delta.
T13-T14	Falling	Constant	Progradation in channels
	Falling	Constant	Progradation, near delta front in channels.
T14-T15	Falling	Constant	Rapid progradation along a large part of the front of the delta.
	Lowstand	Constant	Rapid progradation along a large part of the front of the delta.

Table 2: Summary of observations on the CS experiment.

High frequency supply variation			
Time SL		Q	
T0-T1	Rising	Start fall	Sheetflows over the entire delta, some localized rapid progradation at channels.
	Rising	End fall	Rapidly retrograding sheetflows.
T1-T2	Rising	Start rise	Backstepping of delta.
	Highstand	End rise	Slight progradation from back-step onwards.
T2-T3	Highstand	Start fall	Progradation via lobes positioned mainly at centre of delta front but also to the sides of the delta front.
	Falling	End fall	Progradation via lobes positioned mainly at centre of delta front but also to the sides of the delta front.
T3-T4	Falling	Start rise	Rapid progradation via narrow frequently changing channels
	Falling	End rise	Rapid progradation via narrow channels, progradation fastest in areas with little accommodation space.
T4-T5	Falling	Start fall	Slowing progradation
	Lowstand	End fall	Slow progradation
T5-T6	Lowstand	Start rise	Very slow progradation
	Rising	End rise	Aggradation
T6-T7	Rising	Start fall	Retrogradational sheetflows, sedimentation on large parts of the delta.
	Highstand	End fall	Aggradation via broad channels or sheetflows.
T7-T8	Highstand	Start rise	Progradation in narrow channels on large parts of the delta
	Falling	End rise	Rapid progradation, channels become larger.
T8-T9	Falling	Start fall	Slow progradation on delta front influenced by subsidence, occasionally outside this region.
	Lowstand	End fall	Slow progradation along large parts of the delta through wide channels.
T9-T10	Lowstand	Start rise	Continued progradation, through many simultaneously active channels
	Rising	End rise	Aggradation, on top of last prograding lobes.
T10-T11	Rising	Start fall	Back-step at start run. Sheetflows on large parts of the delta.
	Rising	End fall	Retrogradation and aggradation on the delta in sheetflows.
T11-T12	Rising	Start rise	Back-step at start run. Aggradation through sheetflows on top of back-step.
	Highstand	End rise	Aggradation.
T12-T13	Highstand	Start fall	Slow progradation via small lobes fed by narrow high velocity channels
	Falling	End fall	Slow progradation continues, channels calmer, wider and more stationary.
T13-T14	Falling	Start rise	Progradation through wide channels
	Falling	End rise	Rapid progradation through wide channels, mainly in centre of delta front.
T14-T15	Falling	Start fall	Rapid progradation through channels that frequently change position.
	Lowstand	End fall	Rapid progradation along a large part of the front of the delta.

Table 3: Summary of observations on the HS experiment.

4 Analyses

In this thesis, all information on the CS and HS models and additional analyses on the IP model are presented. The original report on the IP and OP models (Gademan, 2008) can be consulted for the entire analysis of the IP model. Information on the NL and PL models in comparison with the CS model is previously presented as well (de Vries, 2009).

4.1 Lacquer peel analysis: parasequences

Analyses of the CS and HS models are focused on the effects of the frequency variation of discharge. For this purpose, the delta architecture of the delta centre is analysed on the lacquer peel sections (profiles 3 & 4). Observation of the experiments and video analysis shows the most continuous sedimentation at the delta centre. This area has received sufficient accommodation space to limit erosion. Therefore, it is assumed that these sections provide the clearest picture of the differences between the experiments.

Lacquer peels are analysed based on sequence stratigraphy. Separate images are created for parasequences and system tracts. Furthermore, maximum flooding surfaces (MFS) and erosional unconformities (EU) are displayed. To place all observations within a timeframe, timelines are created based on the applied tracers.

Parasequences are subdivided into seven depositional stratotypes. The definition of the different parasequences is based on internal structure and on the migration angle of the roll-over point within parasequences (Figure 6). Both displacement in and in between parasequences describe the effects of supply and sea level variations. The roll-over point migration is considered representative for shoreline migration (Helland-Hansen and Martinsen, 1996).
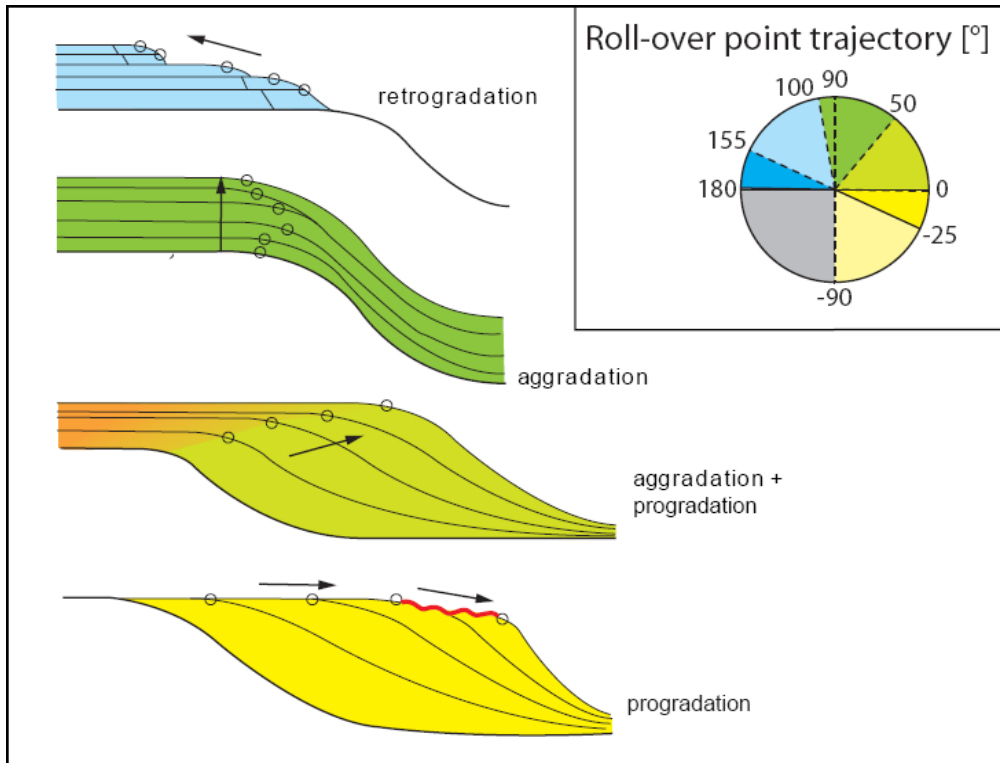

Figure 6: Overview of depositional stratotypes, the colours indicate the different stratotypes. Open dots represent roll-over point migration within one parasequence. Insert: Roll-over point trajectories show the range of different angles possible for each stratotype.

Retrogradational sheet floods

This stratotype is characterised by fast backstepping of strata which is caused by fast sea level rise outpacing the rate of sediment flux. This stratotype does not contain foresets. The roll-over point angle within a retrogradational parasequence ranges from 100º to 155º.

Aggradation

Aggradation is characterised by a balanced sea level rise and sediment flux, resulting in an approximately stationary shoreline. Because of this, aggradational parasequences consist mainly of topsets. Aggradational parasequences can also be associated with onlap on the underlying strata. The roll-over point angle ranges from 50º to 100º.

Progradation

Progradation occurs during a constant or falling sea level. The sediment flux is deposited at the delta front in foresets, topsets are generally reworked. During sea level falls, erosional unconformities are regularly formed on the delta plain. The roll-over point ranges from 0º to -25º.

Aggradation + progradation

This stratotype is an intermediate stratotype in between aggradation and progradation that occurs during sea level rises that are outpaced by the sediment flux. The roll-over point angle within this stratotype ranges from 0º to 50º.

Anastomosing channel fill

Parasequences that are characterised by anastomosing channel fill are of fluvial origin and can be regarded as part of the transport sub-system. This stratotype contains planar horizontal and lensoid channel deposits.

Incised valley fill

Incised valleys form during sea level falls. During subsequent sea level rises, these valleys are filled by horizontally deposited sediments. Occasionally, a sea level fall can be traced throughout the entire delta by incised valley fill sediments.

Toe sets

Toe sets, or subaqueous fans form at high stream power conditions at the delta front and are generally formed at the mouth of narrow channels. Generally, toe sets contain the smallest grain size fraction.

4.2 Lacquer peel analysis: system tracts

In the Exxon sequence stratigraphic model, six system tracts are used to describe delta architecture with respect to the sea level curve (Posamentier et al., 1988; Posamentier and Vail, 1988). However, the PHASE project examines the influence of discharge. If this influence exists, it will alter the relation between the system tracts and the sea level. Therefore, the system tracts cannot be used in terms of the original definition. In this thesis, only transgressive and regressive periods are projected on the lacquer peels based on a clear correspondence to the sea level.
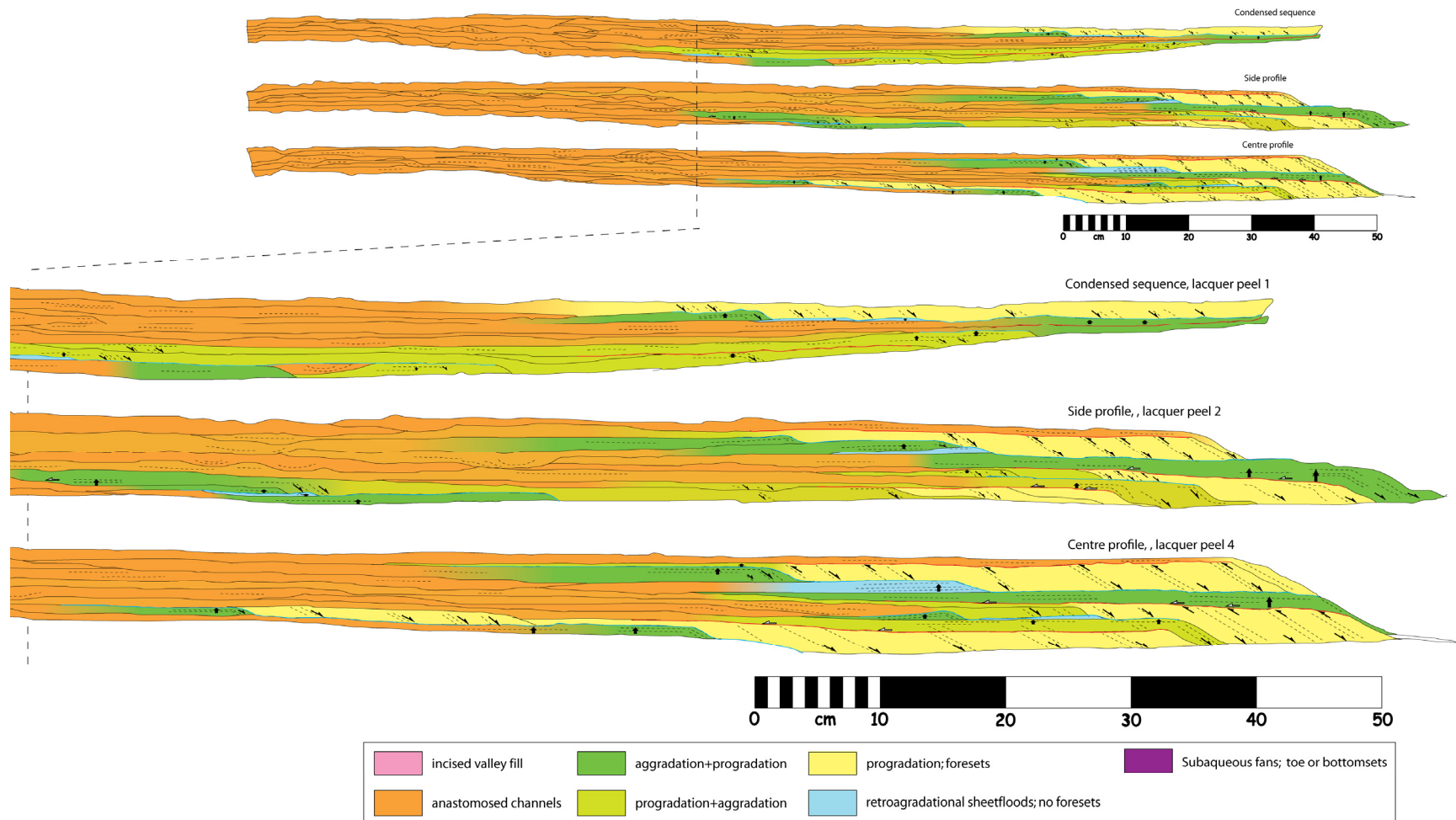
Figure 7: Parasequence analysis of lacquer peels of the CS experiment. The upper picture provides an overview of the entire lacquer peel. A magnification is shown in the lower picture.
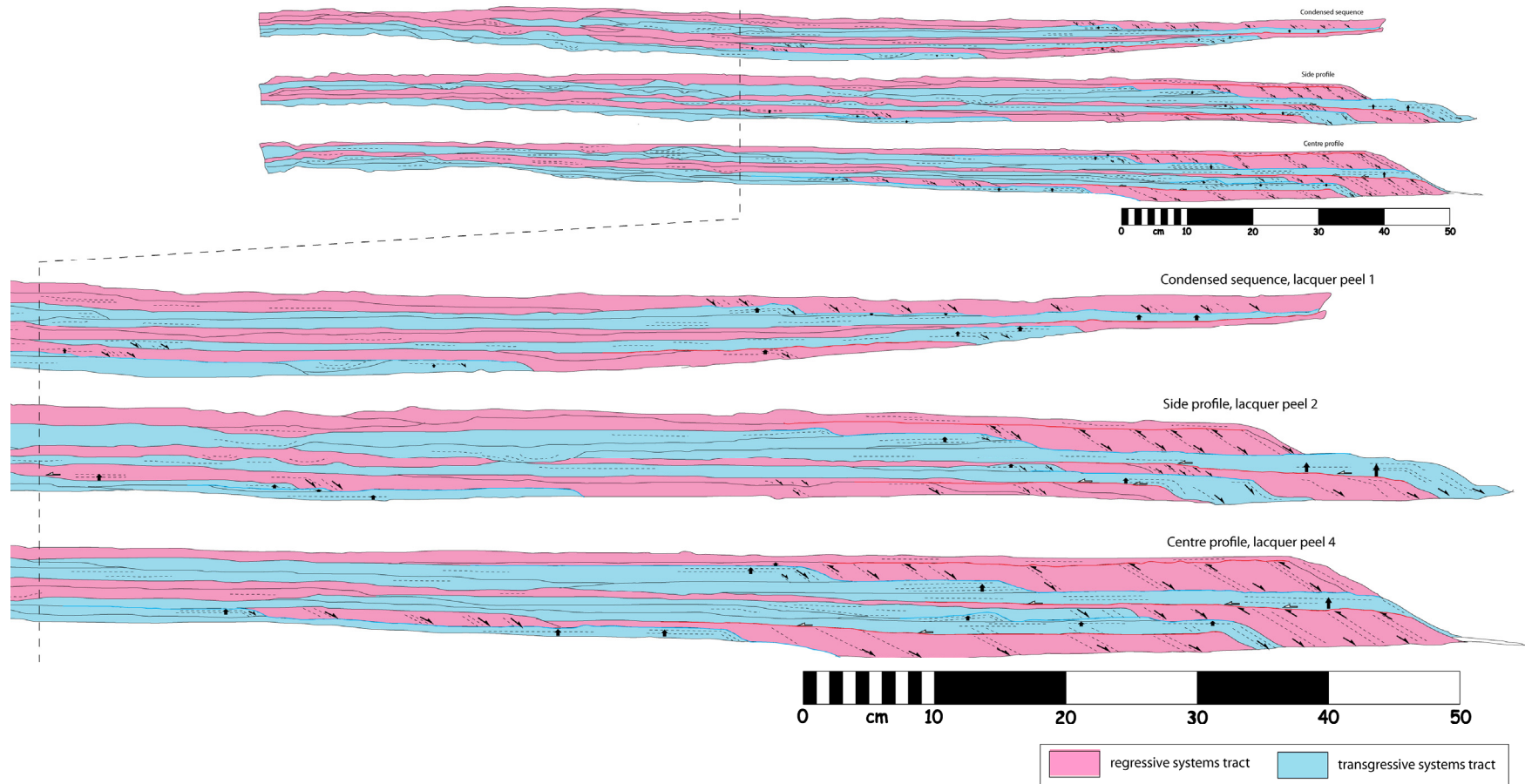
Figure 8: System tracts analysis of lacquer peels of the CS experiment. The upper picture provides an overview of the entire lacquer peel. A magnification is shown in the lower picture.
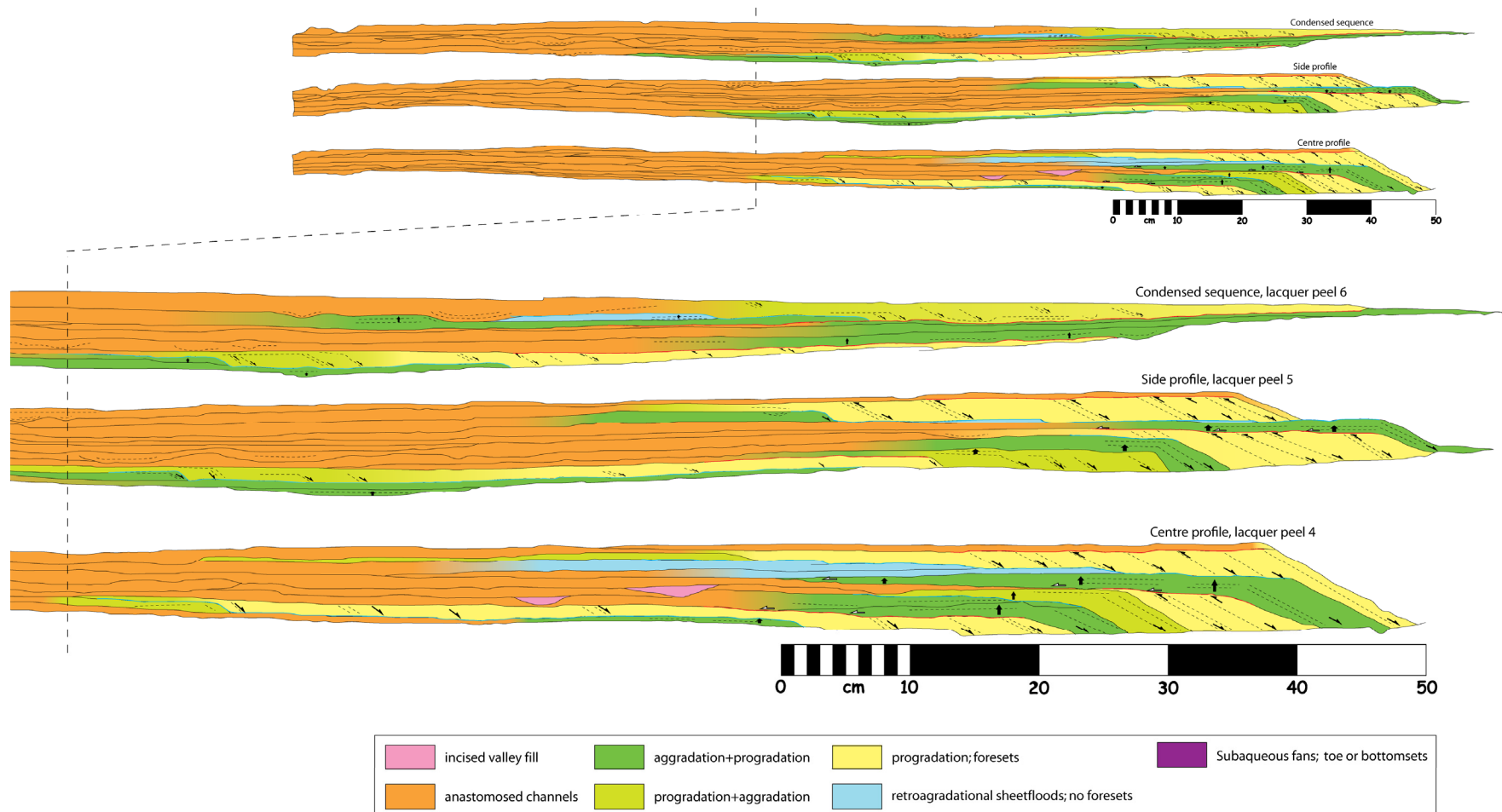
Figure 9: Parasequence analysis of lacquer peels of the HS experiment. The upper picture provides an overview of the entire lacquer peel. A magnification is shown in the lower picture.
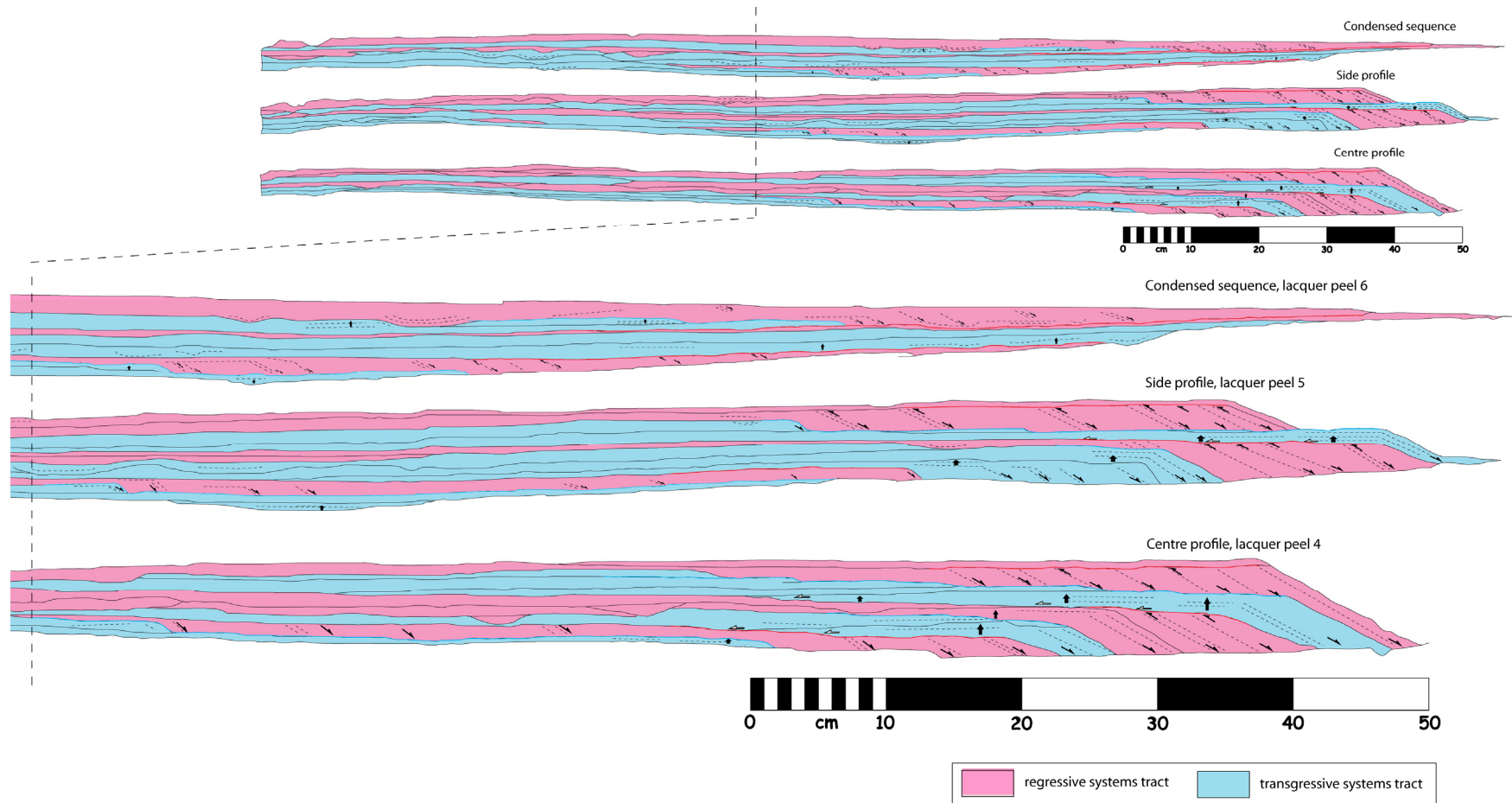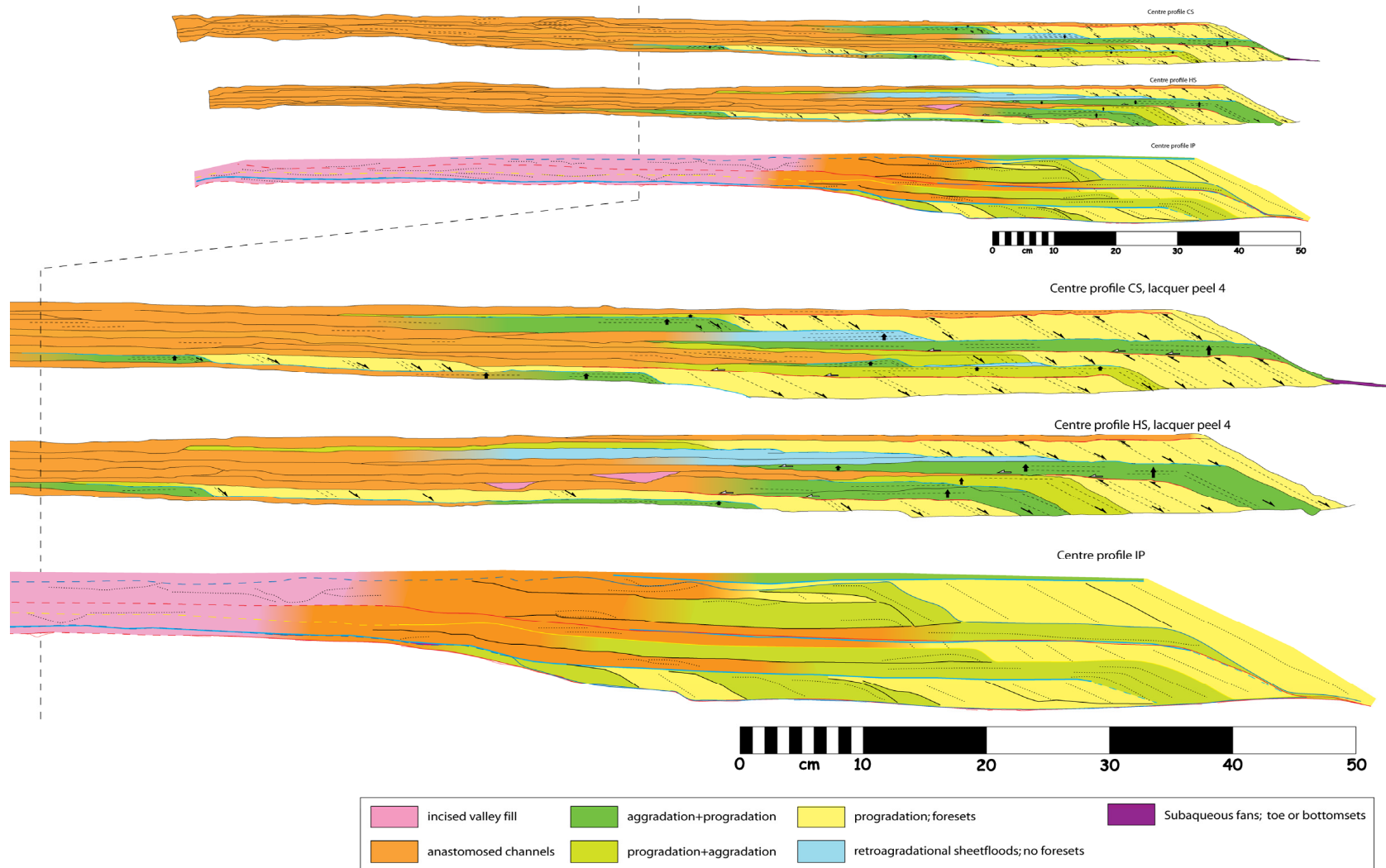
Figure 10: System tracts analysis of lacquer peels of the HS experiment. The upper picture provides an overview of the entire lacquer peel. A magnification is shown in the lower picture.

The impact of climate controlled frequency variations in sediment supply on basin margin architecture

Centre profile CS

Centre profile HS

Centre profile IP

Centre profile CS, lacquer peel 4

Centre profile HS, lacquer peel 4

Centre profile IP

incised valley fill	aggradation+progradation	progradation; foresets
anastomosed channels	progradation+aggradation	retroagradational sheetfloods; no foresets

Subaqueous fans; toe or bottomsets

←**Figure 11: Comparison of parasequence analysis of the centre lacquer peels of the CS, HS and IP experiments. The upper picture provides an overview of the entire lacquer peel. A magnification is shown in the lower picture.**
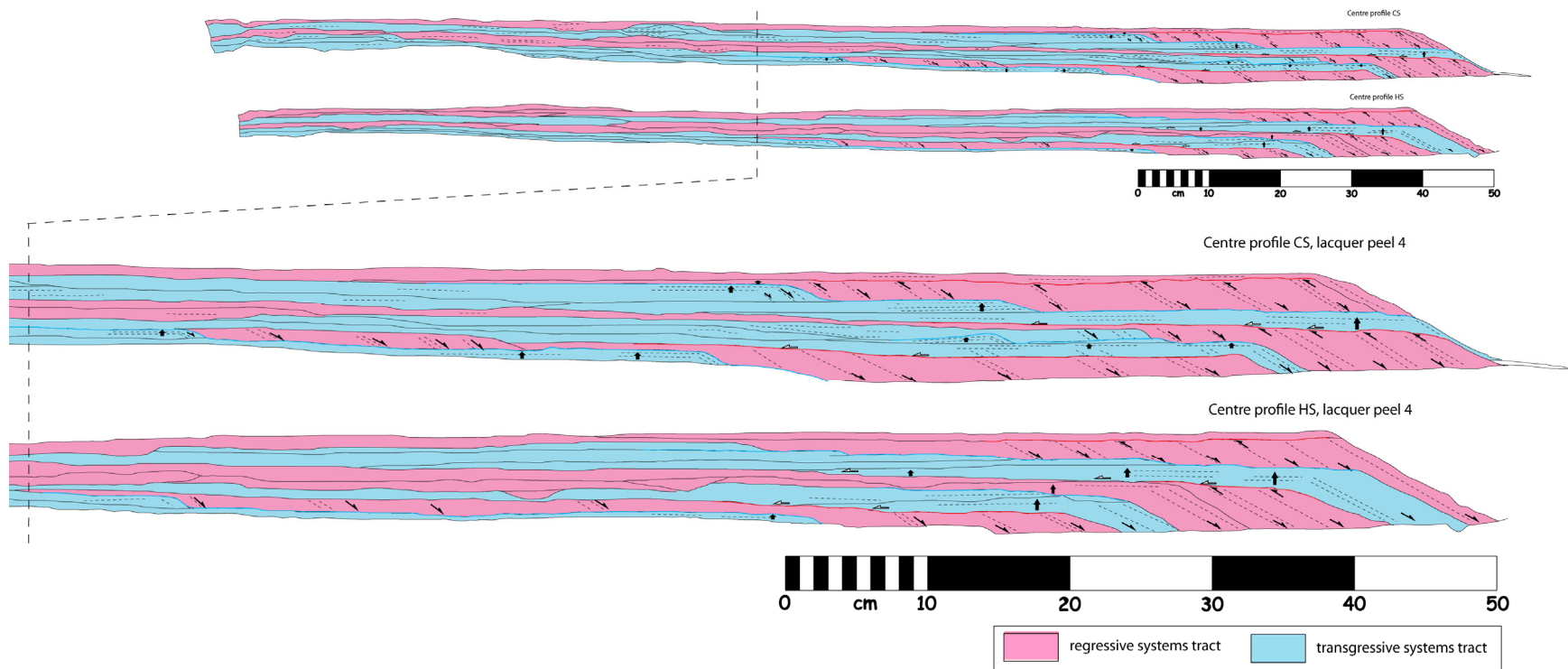

Figure 12: Comparison of system tracts analysis of the centre lacquer peels of the CS and HS experiments. The upper picture provides an overview of the entire lacquer peel. A magnification is shown in the lower picture.

| Sealevel | Timestep | This report | | de Vries, 2009 | | Gademan, 2008 | |
		Constant Supply (CS)	High Frequency Discharge Variation (HS)	Negative Phase Lag Discharge Variation (Q leading on SL) (NL)	Positive Phase Lag Discharge Variation (Q lagging SL) (PL)	In Phase Discharge Variation (IP)	Out of Phase Discharge Variation (OP)
	T0-T1	aggradation	aggradation	aggradation+progradation	retrogradation	aggradation+progradation	aggradation+progradation
	T1-T2	aggradation	aggradation	retrogradation	aggradation	aggradation+progradation	aggradation+progradation
	T2-T3	progradation	progradation	progradation	progradation	progradation	progradation
	T3-T4	progradation	progradation	progradation	progradation	progradation	progradation
	T4-T5	progradation	progradation	progradation	progradation	aggradation+progradation	aggradation+progradation
	T5-T6	aggradation+progradation	aggradation	aggradation	aggradation+progradation	aggradation+progradation	aggradation+progradation
	T6-T7	aggradation	aggradation	aggradation	aggradation	aggradation+progradation	aggradation+progradation
	T7-T8	aggradation+progradation	aggradation+progradation	aggradation	aggradation	progradation	progradation
	T8-T9	progradation	progradaton	aggradation+progradation	aggradation+progradation	aggradation+progradation	aggradation+progradaton
	T9-T10	aggradation	aggradation	aggradation	aggradation	aggradation	aggradation
	T10-T11	retrogradation	retrogradation	aggradation	retrogradation	aggradation	aggradation+progradation
	T11-T12	aggradation	retrogradation	aggradation	aggradation	aggradation+progradation	aggradation+progradation
	T12-T13	aggradation+progradation	aggradation+progradation	progradation	progradation	progradation	progradation
	T13-T14	progradation	progradation	progradation	progradation	progradation	aggradation+progradation
Low High	T14-T15	progradation	progradation	progradation	progradation	progradation	progradation

Table 4: Overview of the different stratotypes of all six PHASE experiments per time step. The CS and HS results are obtained from analyses in this thesis. The IP and OP results are deducted from text and figures in Gademan (2008). The NL and PL results are adapted from a similar figure from de Vries (2009). Sea level fluctuations are included for correlation. Colour coding is based on Figure 6 and included for comparison of the different experiments.

4.3 Architectural differences

<u>Lateral variation within the models</u>

The sea level curve describes three cycles. The second sea level rise is three times smaller than the first and third (Figure 4). Sea level fluctuations are clearly reflected in the centre profiles (profiles 3 & 4, see Figure 5) and the side profiles (profiles 2 & 5), but not in the condensed profiles (profiles 1 & 6). Lacquer peels of the CS model are shown in Figures 7 & 8, and the lacquer peels of the HS model are shown in Figures 9 & 10. For lacquer peels of the IP model see (Gademan, 2008) and Figure 11. All models have three periods during which transgressive system tracts are formed. During these periods, aggradational and retrogradational parasequences are deposited. There are three regressive system tract periods as well, during which generally progradational parasequences are formed. In general, the centre and side profiles within one model describe similar patterns, although the quantitative distribution between parasequences is slightly different. Less accommodation space is available in the side profiles resulting in the more interrupted deposition compared to the centre profiles as is observed on the time-lapse videos as well.

The condensed profiles are not comparable to the other profiles because they are located almost entirely outside the subsidence zone, resulting in condensed sequences. There, accommodation space is very small, resulting in (partial) erosion of the parasequences. The sea level fluctuations are not distinguishable because the timing of the parasequences is unknown. Furthermore, time-lapse video images show a much interrupted record of deposition due to only occasional sedimentation.

<u>Variations between the models</u>

The comparison between the models is focussed on the centre profiles because these are expected to provide the clearest and most consistent results. Comparison between the parasequences and system tracts of the CS and HS models shows significant resemblance (Figures 11 & 12). Although the parasequences in the CS and HS models in general behave similarly, differences are also present (Table 4). In the CS model, progradation during the sea level fall in T2-T5 is significantly more. Thereafter, during T5-T7, the CS model steps back landwards while the HS delta shifts further basinward. During the subsequent sea level fall in T7-T9, the CS model shows more progradation than the HS model. The following sea level rise in T9-T12 results in significant backstepping and drowning of the delta plain in both models. The final sea level fall in T12-T15 is reflected in a similar amount of progradation in both models. Maximum flooding surfaces and erosional unconformities are observed at the same positions in both models. Maximum flooding surfaces are recorded at T2, T7 and T12 and erosional unconformities at T5, T9 and T15.

Comparison between the IP model and other models provides difficulties because of the large apparent differences. Compared to the CS and HS models, the IP model seems provided with a larger amount of subsidence as shown by the outlines of the delta. Furthermore, the internal structure of the

parasequences seems different and less continuous in the IP model. Analysis by another author (Gademan, 2008) might provide analytical inconsistencies in the comparison between the models. However, by focussing on recognition of the sea level curve, comparison is possible. In the IP model lacquer peels only a minor sea level rise is recorded in T0-T2. During these time steps the delta undergoes progradation and aggradation+progradation. Furthermore, the first parasequence starts further basinward. Time steps T0-T5 of the IP model are characterised by progradational and aggradation+progradation parasequences although a maximum flooding surface is recorded at T5. In the CS and HS models an erosional unconformity is recorded at this position. In the IP model, the sea level rise at T5-T7 is reflected in the aggradational+progradational parasequences and the successive sea level fall at T7-T9 by aggradation+progradation and progradational parasequences. In the CS and HS models, this sea level rise is more clearly reflected by aggradational parasequences. At T9 a maximum flooding surface is recorded in the IP model while in the CS and HS models an erosional unconformity is recorded. The successive sea level rise at T9-T12 is reflected by aggradational and aggradational+ progradational parasequences in the IP model. In the CS and HS models, this sea level rise is more clearly recorded by aggradational or even retrogradational parasequences. At T12 another maximum flooding surface is recorded in the IP model which corresponds with the CS and HS models. The subsequent sea level fall is clearly recorded by progradational parasequences, which is similar to the CS and HS models. At the top of T15 a maximum flooding surface is recorded in the lacquer peels of the IP model followed by an aggradational parasequence, while in the CS and HS models an erosional unconformity is recorded formed by anastomosing channels depositing a progradational parasequence at the delta front.

4.4 Quantification of architectural differences: the vector method

To verify the hypothesis that cyclic variations in discharge determine the observed differences in the internal delta architecture (i.e. the amount of progradation or retrogradation), quantification is required. The roll-over point can be used to define transgressive and regressive systems in 2D settings, resulting in a quantitative description of the internal delta architecture (Helland-Hansen and Martinsen, 1996). This method describes the shoreline trajectory by measuring the migration angle between the roll-over points of two successive parasequences (Figure 14a, c). Drawback of this angle method is the low resolution and the inability to distinguish between minor and major variations in roll-over point migration (Figure 13). To recognise the influence of discharge on delta architecture a more precise method is needed.
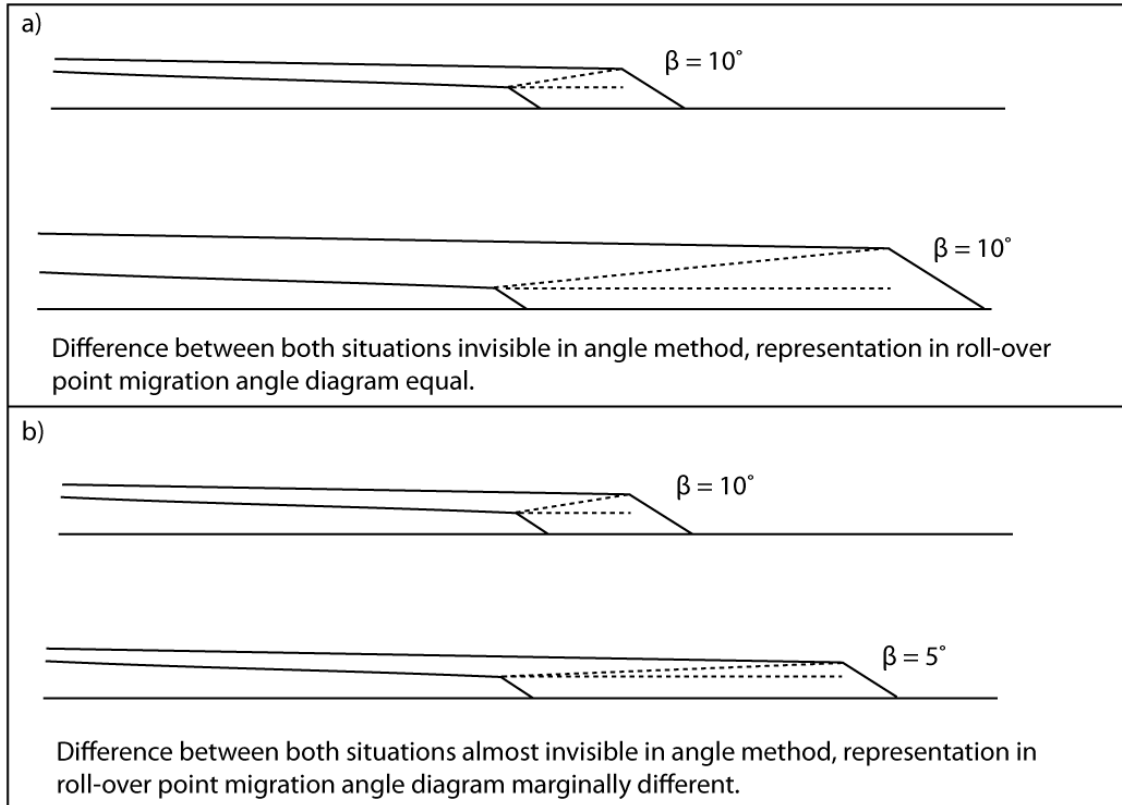
Figure 13: Examples of multiple roll-over point migration trajectories that remain unnoticed in a roll-over point migration angle-representation (Helland-Hansen and Martinsen, 1996). a) Significantly different situations can be represented by an equal angle. b) Much higher sediment input provides only marginally different representation.

A new method to reconstruct 2D roll-over point migration at high resolution will be referred to as the vector method. The vector method is applied by measuring the horizontal and vertical displacement between the roll-over points of two successive parasequences. It is visualized in a bar-type plot (Figure 14b) of distance (x-axis) versus time (y-axis). Both the vertical and horizontal vectors are represented as bars on the x-axis, where horizontal displacement towards the shelf (progradation) and sea level rises are positive. The horizontal vector bar is coloured and the vertical vector bar is gridded. The colours on the horizontal vector bar represent the stratotype of the parasequence (e.g. progradation = yellow). The length of the bars represents the displacement of the roll-over point relative to its previous position. Quasi-3D analysis is possible when multiple sections are constructed and correlated. A comparison of the angle and the vector method is given for the CS model (Figure 16).
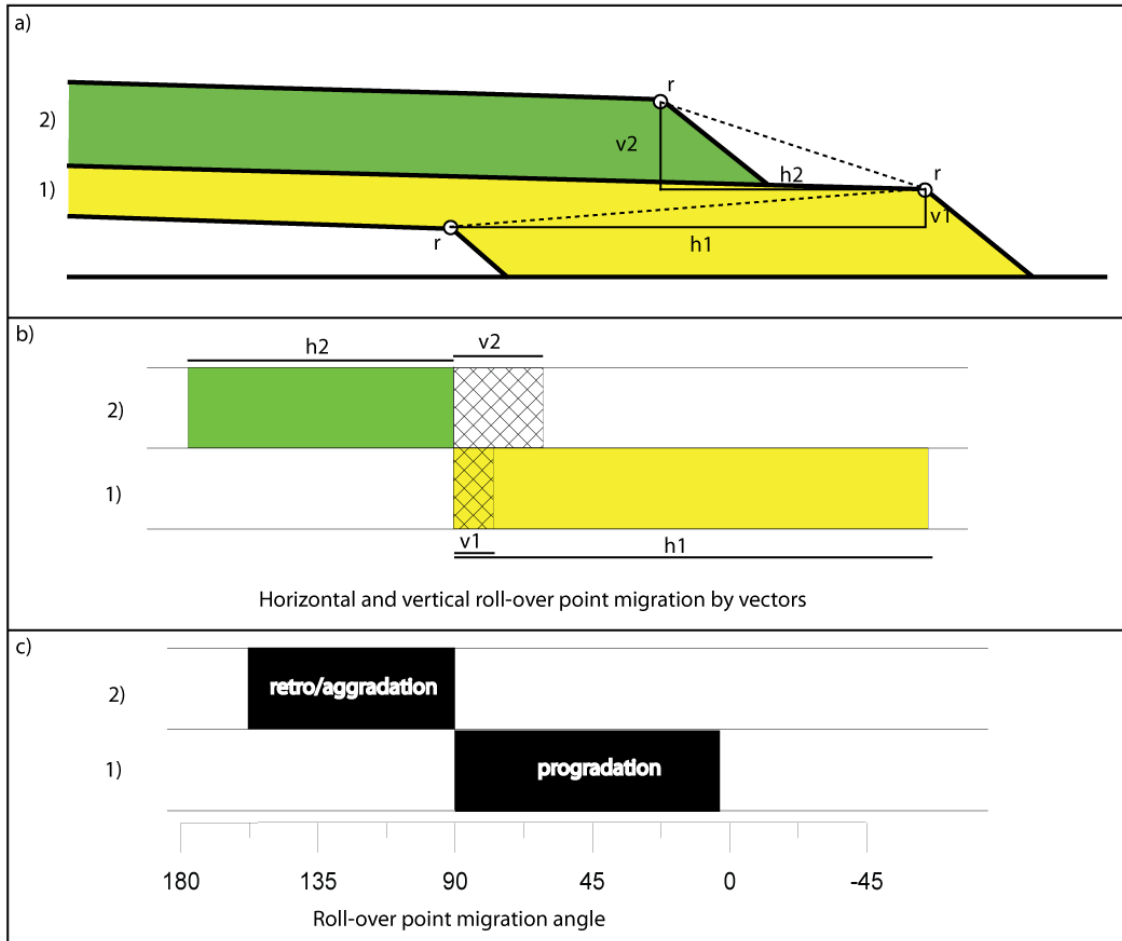
Figure 14: Schematic representation of analysis method. a) Roll-over point migration, r=roll-over points, h=horizontal vector, v=vertical vector. b) Vector method representation, horizontal vector is coloured, vertical vector is gridded. c) Angle method representation (Helland-Hansen and Martinsen, 1996).

The roll-over point migration of the CH, HS and IP models is quantified with the vector method. The necessary data is deducted from the DEM images generated in PETREL. DEM slices are stacked to generate a 2D image of the internal structure of the delta. The sections are equivalent to the centre profiles in the lacquer peels (Figure 6, profiles 3 & 4). The images of the DEM slices can be found in appendix 1 (DVD). All vectors of all models are normalized to the CS model, by setting the value of the largest vector of the CS model to one. This creates a dimensionless scale for comparison of the different models. For the CS, IP and HS models one profile is selected for roll-over point migration vector analysis. The PL and NL models are analysed with the vector method as well (de Vries, 2009). The DEMs data of the OP model is not yet available.

Besides a higher resolution, the vector method has several advantages over the angle method. Firstly, the vertical vector theoretically only describes variations in accommodation space and can therefore be fully related to subsidence and sea level fluctuations. The horizontal vector includes both these factors as well as possible variations in the sediment flux. To verify this, the absolute heights of

the roll-over points of the CS and HS models are measured in the DEMs slices in which subsidence is not yet applied. These absolute heights should correspond to the absolute sea level if this assumption is correct (Figure 15). From Figure 15, it can be concluded that the vertical position of roll-over points is in close correspondence with sea level. Offsets can be explained by multiple causes. (1) Roll-over points closely correspond, but are not equal to sea level. (2) Roll-over points are determined from the DEM slices and therefore it is possible that the roll-over point is determined falsely (e.g. in a channel). (3) Due to the increasing error over time, a systematic error seems likely. Sea level might easily show an offset due to the ~270 successive and relative adjustments during one experiment without absolute control on sea level. However, the offset is relatively small. Therefore the assumption is made that the vertical vector is mainly controlled by sea level and subsidence while the horizontal vector is influenced by sea level, subsidence and sediment flux.

The rate of creation and destruction of accommodation space is largest during high rates of sea level change. Rates of sea level change are given by the derivative of sea level (i.e. sea level gradient, ΔSL). In Figure 16, the sea level gradient is plotted on top of the vector method diagram of the CS model. A close correspondence between the displacement of the roll-over point and the sea level gradient is observed. For the correlation of delta architecture and discharge, the CS, IP and HS centre profiles are fitted with their discharge curves (Figure 17).

The assumption that the vertical vector records sea level and subsidence while the horizontal vector is influenced by discharge as well will be used to subtract the horizontal vectors of the CS model from the HS and IP models. The CS model does not contain a variable discharge influence while all other factors are similar. Therefore, this subtraction will isolate the influence of the discharge scenarios. These difference-graphs are fitted with discharge curves (Q) and the derivative of discharge (i.e. the discharge gradient, ΔQ) (Figures 18, 19 & 20).
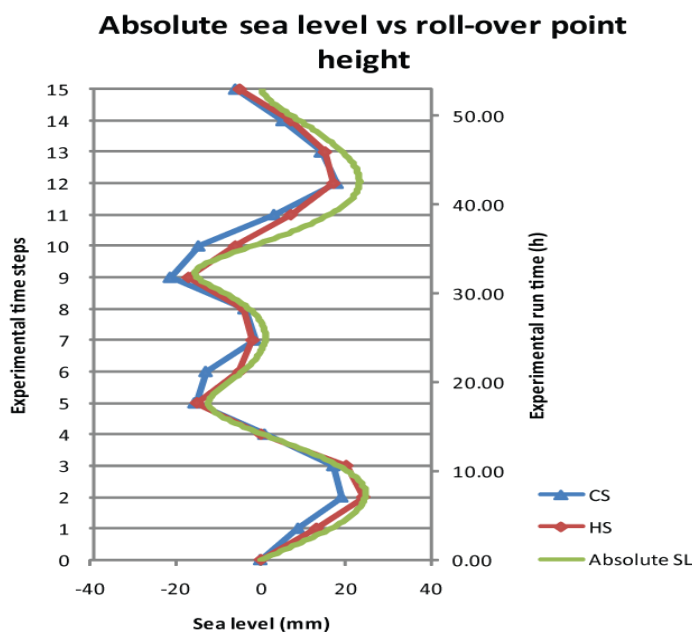

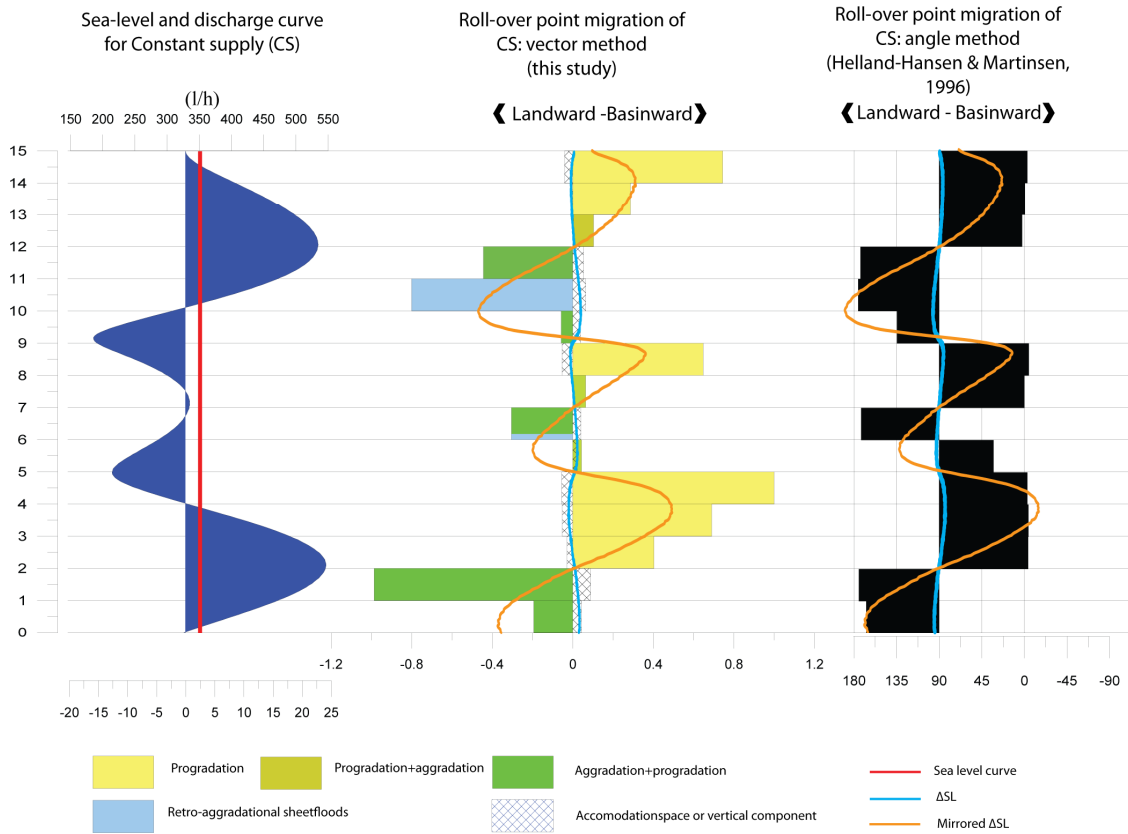**Figure 15: Comparison between input sea level curve and roll-over point positions obtained from DEMs.**

Figure 16: Vector diagram compared to angle diagram (Helland-Hansen and Martinsen, 1996). Both figures are overlain with sea level gradient curves.
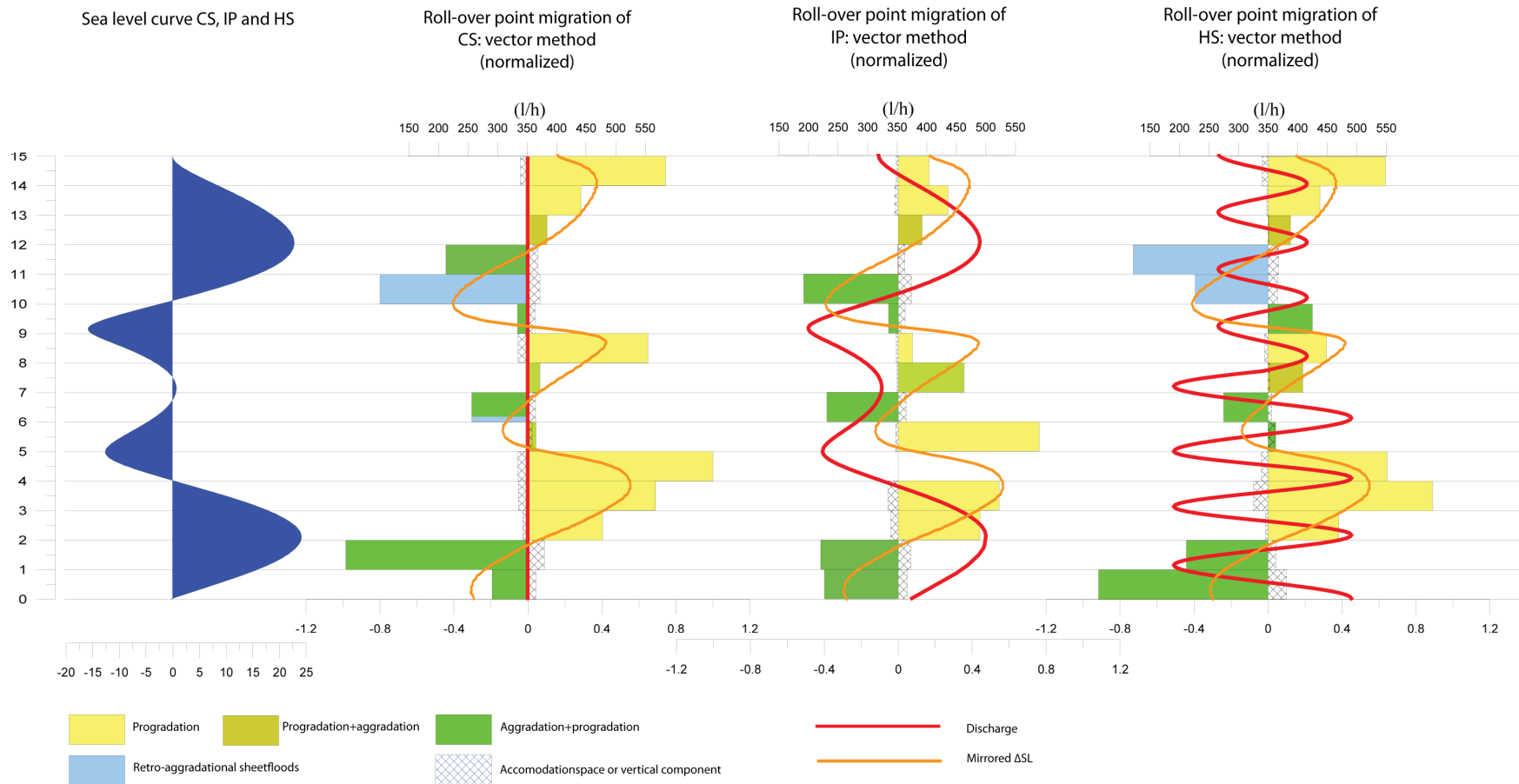
Figure 17: Vector diagrams of CS, IP and HS overlain by discharge and the sea level gradient curve. The horizontal and vertical vectors are normalized by giving the value 1 to the largest vector of the CS model.

Figure 18: Vector diagrams of CS and HS with difference-graph of the horizontal vector overlain by the discharge curve and the discharge gradient curve. The horizontal and vertical vectors are normalized by giving the value 1 to the largest vector of the CS model.
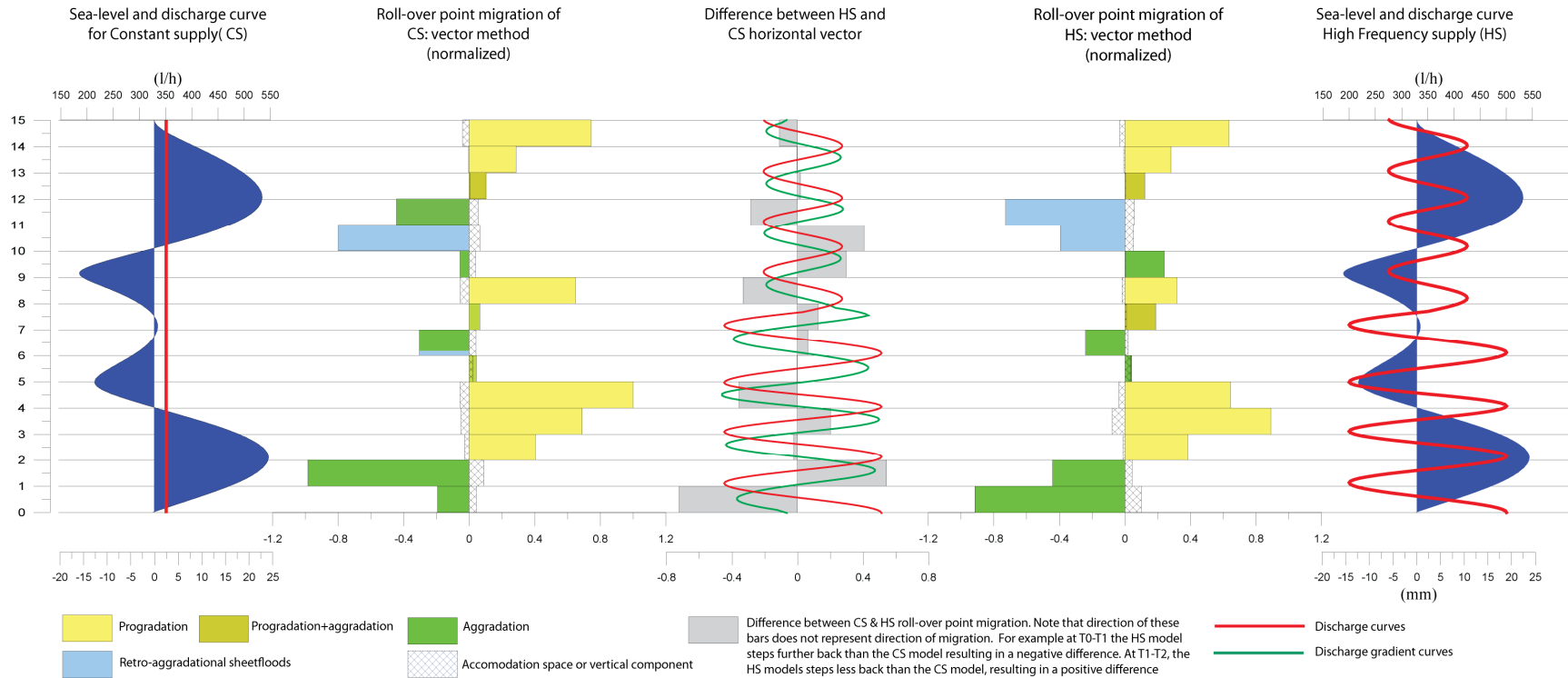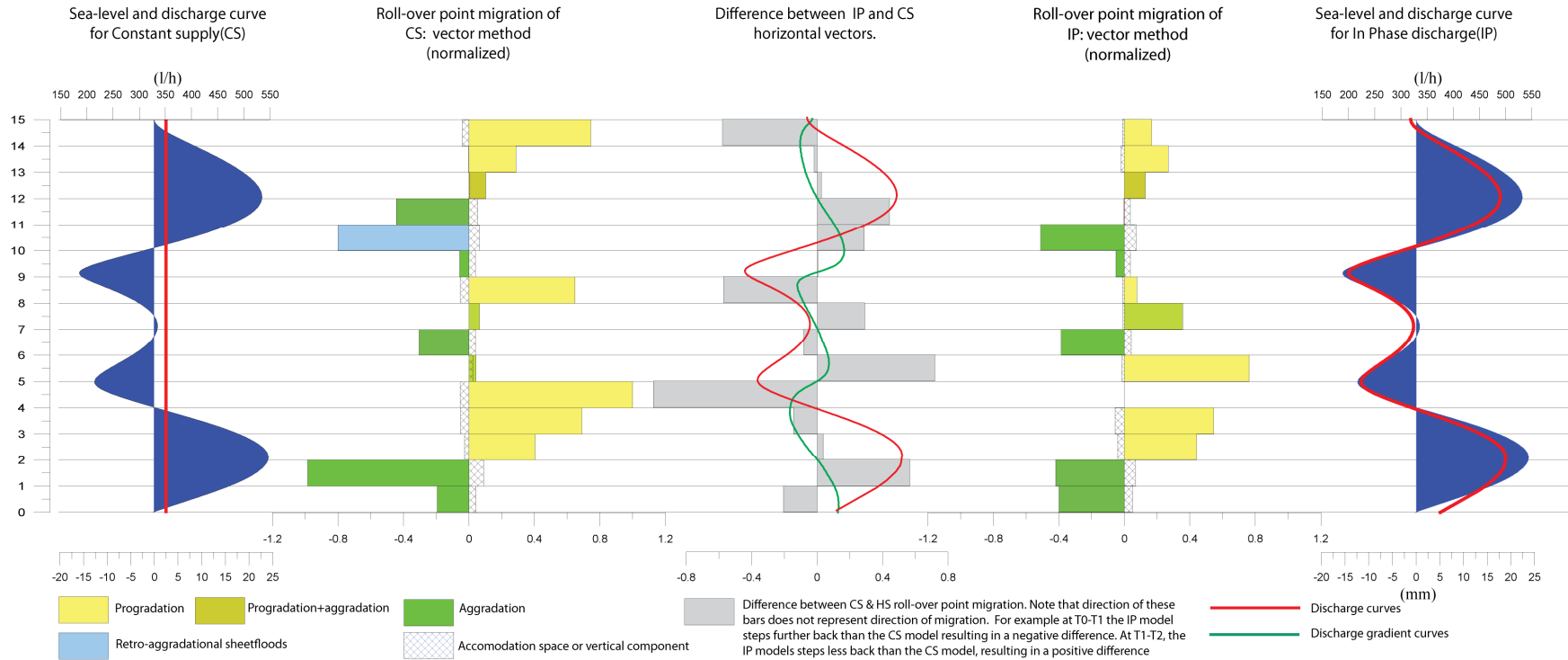
Figure 19: Vector diagrams of CS and IP with difference-graph of the horizontal vector overlain by the discharge curve and the discharge gradient curve. The horizontal and vertical vectors are normalized by giving the value 1 to the largest vector of the CS model.

4.5 Main differences in roll-over point migration

Comparison of the displacement of the horizontal vectors in the IP and HS models with the discharge curves does not reveal a clear correlation. All models however, are in approximate accordance with the sea level gradient curve (Figure 17). One time step (T4-T5) is missing in the IP model. Therefore roll-over point migration is measured between T4-T6. Most likely, most progradation occurred during T4-T5 while aggradation or aggradation+progradation occurred during T5-T6. Therefore, the actual roll-over point migration during these time steps is not properly reflected in the diagram.

The difference-graphs (Figure 18 & 19) show a correlation with the discharge curves although the roll-over points slightly lead over the discharge (Q). The largest differences between the roll-over point migration in the CS model and the HS and IP models are recorded in the discharge curve limbs leading towards peak values instead of on the absolute peaks. The discharge gradient (ΔQ) is plotted as well, leading to another plausible correlation. For the HS model this leads to a positive correlation between roll-over point migration and discharge gradient maxima and minima except for periods T6-T7 and T10-T12, here the opposite correlation applies. The latter time steps correspond to roll-over point positions that could not be determined exactly from the DEM slices. Therefore, the patterns in the diagram might show an offset. The roll-over point migration in time steps T13-T15 shows a very small offset from the CS model. For the IP model, the discharge gradient slightly leads over the roll-over point migration.

5 Discussion

5.1 Offsets in the IP model

The horizontal scale of the IP model is equal to the scales of the CS and HS models. However, the IP delta has almost a double thickness (7 cm vs. 12 cm). This can be explained partially by an error during the appliance of the subsidence at T1, T2 and T3, resulting in a total of 1 cm additional subsidence (D. Mikes, personal communication). This still leaves 4 cm of additional thickness unexplained. Also the external shape of the IP model is different as well. Close to the apex, the thickness of the IP model matches those of the other models but basinward it has an increased thickness. If the appliance of increased subsidence is continued during the entire experiment, both the additional thickness and the different shape are explained. This however is speculation. Another offset is observed in the sediment supply of the IP and OP models. This was at a lower rate of 1.5 l/h vs. 1.65 l/h during the other experiments, resulting in ~10% less sediment input in the IP and OP deltas. The combined effects of additional accommodation space due to increased subsidence and a lower

sediment flux can explain the ~20 cm shorter (apex to delta front) delta and the more stationary position of the roll-over point. Because of these offsets, comparisons of the IP and OP models with the other models might contain a large margin of error.

Furthermore, initial analysis (Gademan, 2008) is not consistent with the vector analysis of the roll-over point migration. Therefore, it is suspected that occasional mistakes are made during lacquer peel analysis. The sea level rise and consequent backstepping of parasequences at T0-T2 is recorded in the DEMs. Therefore, it is suspected that the landward shift has not been correctly interpreted in the lacquer peel analysis (Gademan, 2008). Furthermore, the presence of the MFSs is highly unlikely on top of the progradational part of the sequences (T5, T9, and T15) since MFSs are not recorded at the lowest sea level. Maximum flooding surfaces could only be recorded at these positions if during the transgressions the delta was completely sediment-starved, which is in disagreement with the DEMs. Therefore, it is suspected that terminology is mistakenly used. At positions T5, T9 and T15, erosional unconformities are a more likely surface. This would be in accordance with the delta architecture, the sea level curve, and the other PHASE models.

5.2 Delta architecture

Comparison of the centre profiles of the CS and HS models shows that the delta architecture is mainly determined by sea level and corresponds closely to the sea level gradient curve. However, there are differences in the size of the individual parasequences. The HS model has at each time-step either more or less displacement of the roll-over point position than the CS model. Prime examples of this pattern are time steps T4-T5 & T5-T6 (HS first smaller, than larger) and T7-T8 & T8-T9 (HS first larger, than smaller). This contradicts the hypothesis that short period discharge variations are buffered by river systems (Castelltort and Van den Driessche, 2003). Because the HS discharge scenario consists of only short periods of heightened or reduced discharge, the large scale pattern is very similar to that in the CS model. Therefore, the system tracts, and the positions of erosional unconformities and maximum flooding surfaces are equal to those in the CS model. This is unlike the reported offsets in other discharge scenarios of the PHASE project as previously reported (Gademan, 2008; de Vries, 2009).

Additional caution is taken in the comparison of the CS and IP model to prevent potentially false interpretations because of the previously described offsets and the different representation of the IP lacquer peel analysis (Gademan, 2008). The IP model shows a relatively small horizontal displacement of the roll-over point compared to the CS model. This can be explained by the effects of the IP discharge scenario that is expected to counteract the effects of the sea level curve on delta architecture. High discharge resulting in a high sediment flux is accompanied by high sea level. Low sea level is combined with low discharge, resulting in a relatively stationary roll-over point position. However, this relatively stationary position of the roll-over point can also be explained by the

significantly larger accommodation space available in the IP delta compared to the CS delta. To rule out this possibility, the OP centre profile is consulted (Gademan, 2008) which has a similar subsidence regime as the IP model. In case discharge variations cause the relatively stationary roll-over point patterns, than the OP discharge scenario is expected to have the opposite effect on the roll-over point migration. If subsidence causes the roll-over point patterns, a similar effect is expected for the OP model. The OP model differs significantly from the IP model with larger progradational parasequences suggesting that the OP discharge curve indeed amplifies the effects of the sea level curve. Therefore, the observed patterns in the IP and OP models are most likely caused by the discharge. For the PL and NL scenarios, a correlation is observed between discharge induced variations in the sediment flux and delta architecture (de Vries, 2009).

5.3 The vector method

The vector method as developed for this thesis is an adaptation of the roll-over point migration angle method (Helland-Hansen and Martinsen, 1996). The horizontal and vertical vectors provide a clear and realistically scaled representation of the roll-over point migration. Furthermore, effects of discharge can be isolated with the following assumptions. (1) The vertical vector only describes variations in accommodation space. (2) The horizontal vector is affected by variations in accommodation space and sediment flux. In the PHASE experiment, accommodation space is related to subsidence and sea level fluctuations while the sediment flux is related to discharge. In real passive margin settings, sediment flux is also influenced by other factors such as vegetation which are generally climate related as well on the timescales of interest (10^3 - 10^6yr) (Van der Zwan, 2001).

The effectiveness of the vector method is aptly demonstrated in Figure 16. Here a clear correlation is presented between the horizontal vector and the inversed sea level gradient. This correlation is already made in the Exxon sequence stratigraphic concept (Posamentier et al., 1988; Catuneanu et al., 2009) by linking the rate of creation of accommodation space to the rate of sea level change. However, the direct correlation of roll-over point migration to the sea level gradient curve is made visible with the vector diagram representation, while the correlation cannot be observed clearly in e.g. the angle diagram representation (Helland-Hansen and Martinsen, 1996).

The roll-over point migration vector diagrams of the HS and IP models show a lesser correlation to the sea level gradient curve than that of the CS model. This can be attributed to the discharge scenarios. However, a direct representation of discharge on the vector diagrams does not show a correlation, while the influence of sea level remains visible (Table 4, Figure 17).

The subtraction of the HS and IP horizontal vectors from those of the CS model results in a difference-graph that can be correlated to the discharge curves (Figures 18, 19 & 20). Therefore, the assumptions on the contributing parameters of the horizontal and vertical vector remain valid. The HS

model shows a clear pattern of alternating larger or smaller displacement of the roll-over point than the CS model which was also inferred from the lacquer peels.

5.4 Relation between stream power and the discharge input parameter

The detailed relation between discharge and the roll-over point migration is not straightforward. Generally, sediment carrying capacity is related to stream power and thus indirectly to discharge (Bagnold, 1977; Bagnold, 1980). This leads to the expectancy that maximum stream power and thus sediment carrying capacity is obtained at peak discharge. However the largest differences in roll-over point migration in the HS experiment are obtained at peak values of the discharge gradient instead of peak values of discharge. This discrepancy will be qualitatively explained by the relation between the discharge gradient and stream power. The formula for stream power per unit bed area can be written in several ways (Bagnold, 1977):

$$\omega = \tau\bar{u} = \frac{g\rho QS}{width} \tag{1}$$

With ω = stream power per unit bed area, τ = mean boundary shear stress, $\bar{u}$ = mean flow velocity, g = gravity acceleration, ρ = density, Q = discharge and S = slope. Discharge varies with factor 2.5 (200-500 l/h), observations during the experiment show that slope varies in a similar range. Density is neglected because it varies at orders of magnitude less than discharge and slope. For 2D sections, equation 1 can be rewritten as:

$$\omega = \tau\bar{u} = QS \tag{2}$$

The simplification to a 2D section excludes multiple complications, such as lateral variation and variable channel width. However, the expectation is that these processes only alter the quantitative but not the qualitative relationship that is explained in this thesis.

For simplicity, sea level fluctuations are temporary ignored as well. Furthermore, the roll-over point in pinpointed at a fixed position. In this simple case, a river-delta system that is in an equilibrium state has a constant slope. Therefore, the sediment flux to the delta front is equal to the sediment supply ($S_{out} = S_{in}$). When discharge (Q) is increased, stream power (ω) increases instantaneously in response, while the slope reacts over time. The increased sediment carrying capacity gradually decreases the slope (S), consequently decreasing stream power (ω) as well. The slope is decreased until a new equilibrium is reached. This new equilibrium situation has an equal stream power as the initial equilibrium since the sediment flux must be equal to the sediment supply ($S_{out} = S_{in}$) where sediment supply is fixed at a rate of 1.65 l/h.

At extremes in the discharge gradient curve, the strongest changes in discharge occur. Stream power reacts instantaneous to these discharge changes because the slope can only adjust over time. Therefore, the maxima (and minima) of stream power are obtained on these positive (and negative) peaks in the discharge gradient curve. To reach a new equilibrium, a strong adaptation of the slope is necessary, resulting in a large additional flux of sediment derived from delta plain and river erosion (discharge gradient maxima and stream power maxima) or in a large additional accommodation space at the delta plain and in the river (discharge gradient minima and stream power minima) (Figure 20b). A system that is brought far out of equilibrium, initially adapts rapidly to a new equilibrium because of the large increase in stream power. The final adaptation is extremely slow because stream power is not significantly increased anymore (final ~10% of sediment volume takes ~50% of adaptation time) (Postma et al., 2008). A delta-shelf system is thus able to rapidly respond to strong disequilibria, resulting in a response to the discharge gradient. Previous discharge pulse experiments can be explained via these principles as well (Van Den Berg Van Saparoea and Postma, 2008). Low/moderate discharge changes result in insignificant values in the discharge gradient curve. This does not alter the equilibrium slope significantly per time-step and therefore stream power does not alter significantly as a consequence of a disequilibrium slope angle either. This results in a minor influence of the discharge gradient during low/moderate discharge changes per time step (Figure 20c).

This reasoning is in accordance with computer-modelling studies (Paola et al., 1992). Here diffusivity (discharge) variation is modelled on short timescales (10^4-10^5 yr) where the system is brought out of equilibrium and on long timescales (10^6-10^7 yr) where the system remains approximately in equilibrium. At short timescales maximum progradation was obtained on the rising limb of the discharge curve (Figure 20b), while on long timescales diffusivity did not have effect (Figure 20c). Field results suggesting a dependency on the discharge gradient are obtained from (suspended) sediment dynamics of year-scale discharge variations in large river systems such as the Niger River (Piqouet et al., 2001) and Mississippi River (Mossa, 1996).

Sea level fluctuations shift the equilibrium slope of a river-delta system as well (van Heijst and Postma, 2001). During ice-house conditions, sea level fluctuations have a high frequency and large amplitude resulting in strong peaks in the sea level gradient curve, significantly shifting the equilibrium slope upwards or downwards (Figure 20d).

In reality, variations in sea level and in discharge will generally coincide resulting in interplay between both processes. During ice-house conditions, generally a larger sediment volume is involved in variations induced by the sea level gradient than those induced by the discharge gradient resulting in a dominance of sea level fluctuations in the sedimentary record. A possible exception to this case is provided by strong and rapid variations in discharge which might punctuate or offset larger sea level related trends.

When sea level is the dominant forcing in delta architecture, discharge does have an influence as well because it modulates the time needed for the delta slope to approach the new equilibrium. A

rapid adaptation towards new equilibrium conditions (figure 20d) will be obtained at the high discharge values because of high stream power. A slow adaptation can be expected at low discharge values because of low stream power.
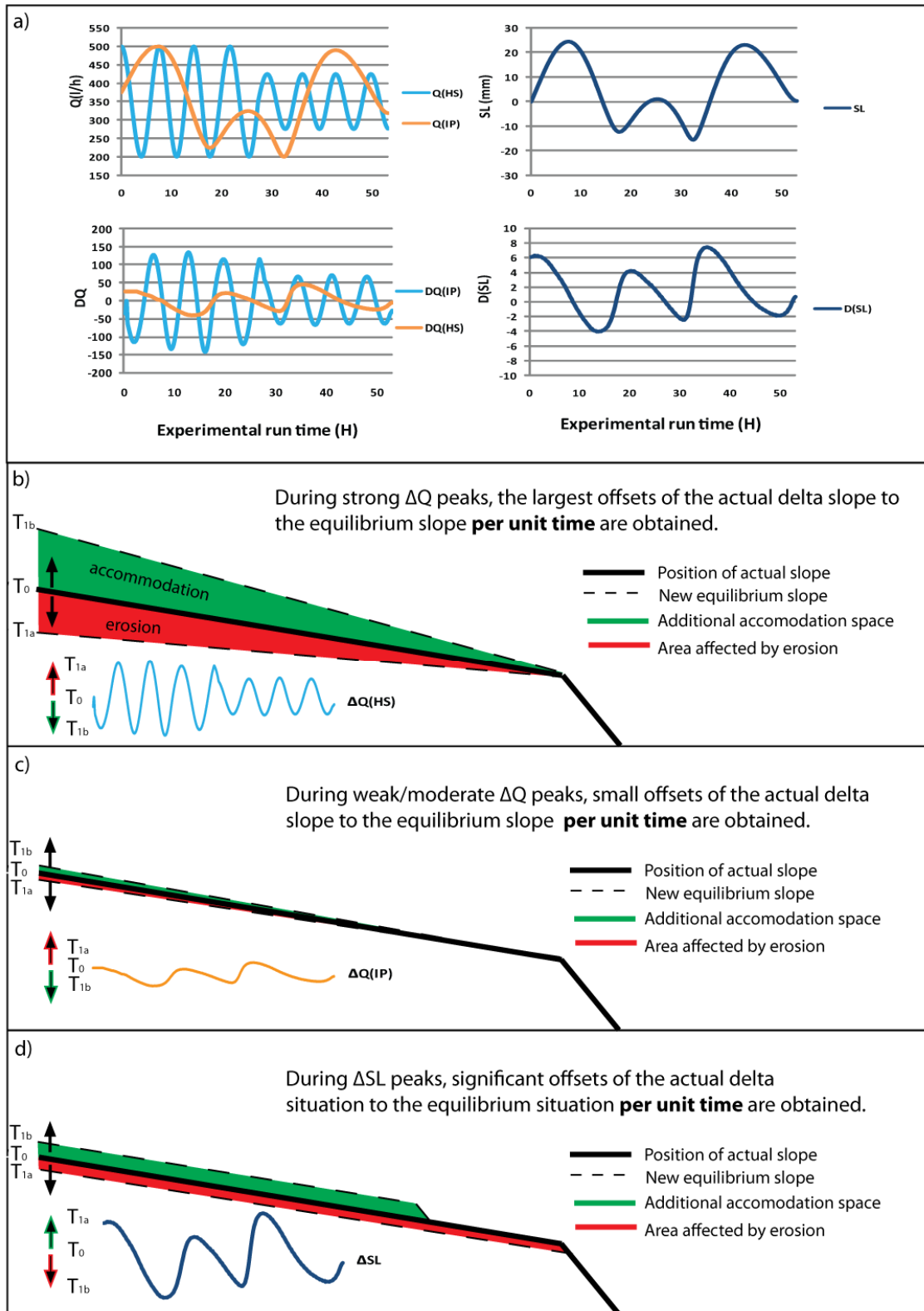
←**Figure 20: a) Discharge and sea level scenarios with their derivatives. b) Graphic display of changes of equilibrium slope per unit time at high rates of discharge change, ΔQ. c) At low rates of ΔQ. d) At ice-house rates of sea level change, ΔSL.**

5.5 The effects of discharge on delta architecture

Application of this reasoning can explain the observations in the HS and IP models. During the first 25 hours of the HS experiment, the frequency of discharge change is approximately three times higher than in the other PHASE experiment scenarios while the amplitude is equal. This results in high peaks in the discharge gradient curve (Figure 20b) and subsequently in a strong adaptation of the equilibrium slope per unit time coinciding with the discharge gradient curve. The frequency of discharge changes in the HS model is approximately three times higher than that of the sea level. Discharge variations are thus the only effect on the equilibrium slope on this timescale, resulting in a clearly visible modulation of roll-over point migration on the longer term sea level forced pattern.

During the second 28 hours of the HS experiment, the frequency of discharge change remains equal but the amplitude becomes twice as low, resulting in lower peak values of the discharge gradient curve. Effectively this leads to only minor disequilibria of the slope of the river-delta system. The amount of additional sediment transported per unit time to reach equilibrium is thus smaller, resulting in a smaller influence of the discharge gradient. Likely, the deviation from the equilibrium state of the river-delta system is also forced by the sea level gradient (Figure 20d). The difference between the roll-over point migration of the CS and HS models is than caused by the modulating effect of discharge itself, resulting in a response to discharge as well in the second 28 hours of the HS experiment.

The IP model has a threefold lower frequency of discharge variation than the first half of the HS experiment, resulting in three times lower discharge gradient peaks. The difference-graph of the roll-over point migration shows a slight lead on the minima and maxima of the discharge curve (Figure 19), suggesting only a minor influence of the discharge gradient on roll-over point migration. The sea level and discharge curve have the same frequency; therefore it is likely that primarily the sea level gradient forces adaptations of the equilibrium slope. The deviation between the roll-over point migration of the CS and IP models is caused by the adaptation-time toward the new equilibrium which is determined by the low or high discharge during the specific time step. Therefore, discharge slightly modulates the effects of sea level, resulting in a response to discharge in the difference-graph.

The response to discharge variations is thus not similar in each scenario. During high frequency and amplitude variation, resulting in high peaks in the discharge gradient curve, disequilibrium of the river-shelf system is forced by variations in discharge. This results in a correspondence between the discharge gradient curve and the strongest offset from the CS roll-over point migration. At lower frequency and amplitude, the sea level gradient is the dominant process in altering the equilibrium state of the river-delta system, resulting in a modulation of the sediment flux

by discharge itself. In these cases, the discharge curve correlates with the strongest offset from the CS roll-over point migration.

The emphasis in the PHASE project is on discharge variations during icehouse periods. Next to influences from discharge, a dominant influence from sea level variations is observed during these periods. During greenhouse periods however, these sea level fluctuations are smaller and more gradual. Therefore it is very likely that discharge variations are the dominant control on deltas during greenhouse periods.

5.6 Field application

Recognition of climate influences on delta architecture in real world passive margin deltas is difficult. Most likely, the climate influences are most clearly recorded by discharge induced effects on the sediment flux because discharge variations provide a rapid mechanism that is least likely to be attenuated (Schlager, 1993; Leeder et al., 1998).

To create a better understanding of these discharge effects, they are preferably first studied during periods of insignificant eustatic variation because climatic effects are probably the dominant control on delta architecture during such periods. During ice-house conditions, delta architecture is dominantly controlled by sea level fluctuations. Therefore, a detailed sea level curve, constructed independently from eustatic observations in deltas, is needed to isolate a possible climate influence (e.g. Miller et al., 2003, Miller et al., 2005). Furthermore, a high resolution time frame is needed to determine the correlation between individual (para)sequences and the sea level curve. Subsequently, the vector method for roll-over point migration can be applied in field research or in seismic interpretation in a similar fashion as the angle method (Helland-Hansen and Martinsen, 1996). According to the results of the PHASE project, the derivative of the sea level curve provides a good baseline for a situation without climatic effects. Significant cyclic offsets from this baseline are probably climate related.

A delta fed by a small river system is the preferred subject of research. These systems are less likely to bypass the shelf, are less affected by sediment routing, and are generally less complex. Large rivers generally have large drainage areas that might contain multiple climate signals. Furthermore, multiple sea level cycles should be recorded to quantify the effects of discharge and sea level variations. Ideally, field or seismic sections of deltas are situated in a region with a climate regime similar to the HS model. In this analogue model discharge forcing is on a higher frequency than sea level forcing, providing the clearest discharge signal.

Previous research on the Spitsbergen deltas provides a good starting point for the field-verification of the PHASE experiment results. Deltaic sediments in the Central Basin of Spitsbergen range from the Barremian to the Eocene (Steel et al., 2000; Plink-Björklund, 2005). During this period, greenhouse conditions prevailed, probably resulting in well recorded climate signals within

the deltaic sediments. These deltas are continuously exposed from the coastal plain to the marine domain. Sediments are generated approximately 25-30 km away in the West-Spitsbergen fold and trust belt. Therefore, the river transport length and time are very short. The entire system is also located in one climate zone, providing an excellent section to determine climate influences. Roll-over point measurements could be obtained from previous research (Steel et al., 2000; Plink-Björklund, 2005 and references herein). A high resolution time-frame could be obtained from stratigraphic markers (Plink-Björklund and Steel, 2005) and integrated stratigraphy, including magneto-, bio- and possibly cyclo-stratigraphy. Generally, continuous stratigraphic sections are not available in deltaic deposits. However, because deltaic sediments are 'walked out' into deep marine sequences (Plink-Björklund, 2005) a continuous stratigraphic section must be possible. Therefore, the Spitsbergen deltas meet the criteria for detailed research on climate components in delta architecture.

The understanding of climate influence on delta architecture might also provide a better understanding on turbidite formation. Generally, the formation of turbidite deposits is linked to falling stage or lowstand stage deltas in sequence stratigraphy. Preferably, deltas are situated on a narrow shelf enabling the progradation of deltaic sediments beyond the shelf-edge (Vail et al., 1977; Posamentier et al., 1988). However, studies have shown that under certain circumstances shelf bypass is possible during the highstand stage (Carvajal and Steel, 2006; Covault et al., 2007). The driving mechanism in these highstand stage situations is not yet determined since rapid sea level changes are unlikely (Sømme et al., 2009). High frequency sediment flux pulses induced by strong discharge variations might provide a (partial) explanation for this situation (Burgess and Hovius, 1998). This topic can be integrated in the research on Spitsbergen deltas, as turbidite deposits are documented here as well (Plink-Björklund et al., 2004; Johannessen and Steel, 2005).

Other possible starting points are deltas with a well-understood and drastically varying climatic regime. Examples are deltas forced by the Asian and North-African monsoonal systems. Previous research has shown that a climate component is present in the Ganges deltaic sediments (Goodbred Jr., 2003) and Indus fan sediments (Prins et al., 2000). These systems however are extremely large and dominated by suspended sediment load, making them less suited to verify the PHASE experiment results or apply the newly developed vector method. Better suited are small, coarse grained deltas (Postma, 2001). An example of such a delta is the Mediterranean Ebro delta (Field and Gardener, 1990; Dañobeitia et al., 1990).

5.7 Adjustments to the Exxon sequence stratigraphic model

The PHASE project was devised to examine whether the Exxon sequence stratigraphic model is valid or whether it should be adapted to include discharge influences. During the experiments, sea level variations provided a dominant control on delta architecture although a distinguishable influence of discharge is observed.

However, the strength and timing of discharge influence is dependent on both amplitude and frequency of discharge changes, their mutual relation (Postma et al., 2008; this thesis), and on their relation to sea level fluctuations (this thesis). Furthermore, discharge-scenarios with either buffering or enhancing effects on sea level can be imagined. Currently, the sequence stratigraphic model can be applied on all deltas influenced by sea level variations. Including discharge poses a major challenge because the sequence stratigraphic model has to be applicable to a significant amount of deltas to remain useful. Discharge is not a necessity in the sequence stratigraphic model because predictions are fairly accurate without it, although it would be an improvement on the Exxon sequence stratigraphic model if it can be included in a workable method. A possible middle course is to classify river-delta systems in a small number of climatic regimes (e.g. with long term climate models), increasing the predictive power of the sequence stratigraphic model while maintaining its general usability. Each of these zones can be provided with a standard sequence stratigraphic model including a discharge component. An example zone is the monsoon affected regions. Climate responses in these systems are on a precession timescale, resulting in high amplitude and frequency discharge pulses that possibly modulate the longer, eccentricity time scale sea level responses (Goodbred Jr., 2003). To include climate of the geological past should be possible because it is reasonably constrained by Milankovitch forcing (e.g. Laskar et al., 2004). If a climatic regime is combined with basic knowledge of the tectonic setting and geographic position of a catchment, river and delta, discharge might be included in a generally useful manner.

6 Conclusions

The PHASE project consists of six analogue flume-tank models of river-delta systems with six different discharge scenarios to examine the validity of the Exxon sequence stratigraphic concept during ice-house conditions. The models are analysed by 2D lacquer peel interpretation and roll-over point migration. The latter analysis is performed with the vector method, a new representation of data that reveals clear results that are not previously reported.

In the PHASE experiment only discharge and sea level determine the delta architecture. When sea level is the only variable parameter, the vector method shows a clear correlation between the roll-over point migration and the rate of sea level change. This correlation is in correspondence with previous findings that link the rate of eustatic change to the availability of accommodation space.

Discharge provides another controlling parameter on the delta architecture. Discharge variations affect delta architecture in two ways: 1) by rates of discharge change / discharge gradient (ΔQ), and, 2) by absolute values of discharge (Q).

At high frequency and high amplitude discharge changes, the discharge gradient pushes a delta slope significantly out of equilibrium per unit time. This results in peak values of stream power

at these occasions, subsequently causing short period sediment pulses in response to the discharge gradient. These pulses can be distinguished in the delta architecture because they operate on shorter timescales than sea level variations, therefore causing punctuations on the longer term sea level forced trend. Consequently, short period discharge pulses are not buffered by river systems.

Discharge is important because it determines the sediment carrying capacity via stream power when eustatic variations force the disequilibrium of the slope. At low/moderate rates of discharge change (high amplitude and a frequency equal to rate of sea level change), the disequilibrium of the delta slope caused by the discharge gradient is minor. Disequilibrium of the delta is dominantly forced by the rate of sea level fluctuations. In this case, discharge modulates the time needed for the delta slope to approach the new equilibrium, resulting in a response to discharge. When operating on the similar time scale as sea level fluctuations, the influence of discharge is more difficult to distinguish but remains present. In real world scenarios, discharge is linked to climate. Therefore, climate becomes a factor that needs considering during assessment on deltaic systems.

According to the results on discharge frequency variation in the PHASE project, the Exxon sequence stratigraphic concept remains valid. The addition of a climate component would increase the predictive power of the model. However, it poses a major challenge to include this parameter because of its complexity. Sea level fluctuations remain dominant thus the addition of a climate component provides only a moderate improvement.

Recommendations

The PHASE project has yielded a highly detailed and elaborate data-set. Therefore, not all data has yet been included in this thesis. Only when all data of all six analogue models is included, final conclusions can be drawn. The vector method needs additional evaluation on its benefits and disadvantages when it is compared to other methods, although the expectancy is that it will proof to be effective. The flume experiments should also be repeated with, for example, different sea level curves to verify whether the observed relations can be obtained with different input parameters as well. Furthermore, the hypothesis on the influence of the discharge gradient can and needs to be examined and verified with slope-angle measurements from the height model data of the HS experiment. However, since height model information is only available on maxima and minima of the discharge curve, the resolution most likely is too low for confirmation or rejection of this hypothesis. Therefore, in successive experiments on the influence of discharge, DEMs should be generated at preferably three times higher time-resolution, enabling the unravelling of the relation, timing and effects of discharge, sea level and delta architecture.

Acknowledgements

References

Abels, H.A., Hilgen, F.J., Krijgsman, W., Kruk, R.W., Raffi, I., Turco, E., and Zachariasse, W.J., 2005, Long-period orbital control on middle Miocene global cooling: Integrated stratigraphy and astronomical tuning of the Blue Clay Formation on Malta, *Paleoceanography, 20*, 1-17.

Bagnold, R. A., 1977, Bed Load Transport by Natural Rivers, *Water Resources Research* 13, 2, 303-312

Bagnold, R. A., 1980, An Empirical Correlation of Bedload Transport Rates in Flumes and Natural Rivers, *Proceedings of the Royal Society of London. Series A, Mathematical and Physical Sciences* 372, 453-473

Burgess, P.M. and Hovius, N., 1998, Rates of delta progradation during highstands: consequences for timing of deposition in deep-marine systems. *Journal of the Geological Society of London* 155, pp. 217–222.

Carvajal, C.R., and Steel, R.J., 2006, Thick turbidite successions from supply-dominated shelves during sea-level highstand: *Geology*, 34, 665–668.

Castelltort, S., and Van den Driessche, J., 2003, How plausible are high-frequency sediment supply-driven cycles in the stratigraphic record? *Sedimentary Geology*, 157, 3-13.

Catuneanu, O., V. Abreu, J.P. Bhattacharya, M.D. Blum, R.W. Dalrymple, P.G. Eriksson, C.R. Fielding, W.L. Fisher, W.E. Galloway, M.R. Gibling, K.A. Giles, J.M. Holbrook, R. Jordan, C.G.St.C. Kendall, B. Macurda, O.J. Martinsen, A.D. Miall, J.E. Neal, D. Nummedal, L. Pomar, H.W. Posamentier, B.R. Pratt, J.F. Sarg, K.W. Shanley, R.J. Steel, A. Strasser, M.E. Tucker and C. Winker, 2009, Towards the standardization of sequence stratigraphy, *Earth-Science Reviews* 92, pp. 1–33.

Clemens S.C., Murray D.W., Prell W.L., 1996, Nonstationary phase of the Plio-Pleistocene Asian monsoon, *Science*, 274, 943– 948.

Covault, J.A., Normark, W.R., Romans, B.W., and Graham, S.A., 2007, Highstand fans in the California Borderland: The overlooked deep-water depositional systems: *Geology*, 35, 783–786.

Dañobeitia, J.J., Alonso, B. and Maldonado, A., 1990, Geological framework of the Ebro continental margin and surrounding areas. In: Nelson, C.H. and Maldonado, A., Editors, 1990. *The Ebro margin Marine Geology, 95*, 265–287.

de Vries, J., 2009, The control of the timing of climate change relative to sea level change on basin margin architecture, Master Thesis, Faculty of Geosciences, Utrecht University

Field, E. and Gardener, V., 1990. Pliocene–Pleistocene growth of the Rio Ebro margin, northeast Spain: a prograding-slope model. *The Geological Society of America Bulletin* 102 6, pp. 721–733.

Gademan M., 2008, Differences between in-phase and out-phase delta systems, Bachelor thesis, Faculty of Geosciences, Utrecht University

Goodbred Jr., S.L., 2003, Response of the Ganges dispersal system to climate change: a source-to-sink view since the last interstade, *Sedimentary Geology 162,* 83-104.

Hays, J.D., Imbrie, J. and Shackleton, N.J., 1976, Variations in the earth's orbit: Pacemaker of the ice ages. *Science,* 194 , 1121–1132.

Helland-Hansen, W., and Martinsen, O.J., 1996, Shoreline trajectories and sequences: description of variable depositional dip scenarios, *Journal of Sedimentary Research*, 66, 670-688.

Imbrie J. and Imbrie J.Z., 1980, Modeling the climatic response to orbital variations. *Science,* 207, 943–953.

Jervey, M.T., 1988, Quantitative geological modeling of siliciclastic rock sequences and their seismic expression, in Wilgus, C.K., Hastings, B.S. and eds., *Sea level changes - an integrated approach, Volume 42: Special Publication, Society of Economic Paleontologists and Mineralogists*, p. 47-68.

Johannessen, E.P., and Steel, R.J., 2005, Shelf-margin clinoforms and prediction of deepwater sands: *Basin Research*, 17, 521–550

Kirkby, M.J., Cox, N.J., 1994. A climatic index for soil erosion potential (CSEP) including seasonal and vegetation factors. *Catena* 25, 333– 352.

Langbein, W.B., Schumm, S.A., 1958. Yield of sediment in relation to mean annual precipitation. *Transactions - American Geophysical. Union* 39(6), 1076–1084.

Laskar, J., Robutel, P., Joutel, F., Gastineau, M., Correia, A.C.M., and Levrard, B., 2004, A long-term numerical solution for the insolation quantities of the Earth, *Astron. Astrophysical,* 428, 261-285.

Leeder, M.R., Harris, T., and Kirkby, M.J., 1998, Sediment supply and climate change: implications for basin stratigraphy, *Basin Research*, 10, 7-18.

Meijer, X.D., 2002, Modelling the drainage evolution of a river-shelf system forced by Quaternary glacio-eustacy, *Basin research*, 14, 361-377.

Meijer, P.Th., and E. Tuenter, 2007, The effect of precession-induced changes in the Mediterranean freshwater budget on circulation at shallow and intermediate depth, *J. Mar. Sys.*, 68, 349-365.

Miller, K.G., Sugarman, P.J., Browning, J.V., Kominz, M.A., Hernández, J.C., Olsson, R.K., Wright, J.D., Feigenson, M.D., and Van Sickel, W., 2003, Late Cretaceous chronology of large, rapid sea-level changes: Glacioeustasy during the greenhouse world: Geology, 31, 585–588.

Miller, K.G., Kominz, M.A., Browning, J.V., Wright, J.D., Mountain, G.S., Katz, M.E., Sugarman, P.J., , Pekar, S.F., 2005, The phanerozoic record of global sea-level change, *Science*, 310 , 1293-1298,

Mossa, J., 1996, Sediment dynamics in the lowermost Mississippi River, Engineering Geology, 45, 1-4, 457-479,

Muto, T., and Steel, R.J., 1997, Principles of regression and transgression: the nature of the interplay between accommodation and sediment supply, *Journal of Sedimentary Research*, 67, 994–1000

Nesbitt,W. H., Fedo C. M, 1997, Quartz and Feldspar Stability, Steady and Non-steady-State Weathering, and Petrogenesis of Siliciclastic Sands and Muds, *Journal of Geology*, 105, 2, 173, 19p

Paola. C., Heller P. L. Angevine C. L. 1992, The large scale dynamics of grain-size variation is alluvial basins, 1: Theory, *Basin research*, 4, 73-90.

Picouet, C., Hingray, B., Olivry, J. C., 2001, Empirical and conceptual modelling of the suspended sediment dynamics in a large tropical African river: the Upper Niger river basin, *Journal of Hydrology*, 250, 1-4, 19-39.

Plink-Björklund, P., Steel, R.J., 2004. Initiation of turbidity currents: outcrop evidence for Eocene hyperpycnal flow turbidites. Sedimentary Geology 165, 29–52.

Plink-Björklund, P., 2005, Stacked fluvial and tide-dominated estuarine deposits in high-frequency (fourth-order) sequences of the Eocene central Basin, Spitsbergen. *Sedimentology* 52: 391–428.

Plink-Björklund, P. and Steel, R., 2005, Deltas on falling-stage and lowstand shelf margins, Eocene Central Basin of Spitsbergen: Importance of sediment supply. In: River Deltas–Concepts, Models and Examples (Eds J. Bhattacharya and L.Giosan), *SEPM Spec. Publ*., 83, 179–206.

Posamentier, H.W., Vail, P.R., Wilgus, C.K., and Hastings, B.S., 1988, Eustatic controls om clastic deposition II - Sequence and systems tract models. In: C.K. Wilgus, B.S. Hastings, C.G.St.C. Kendall, H.W. Posamentier, C.A. Ross and J.C. Van Wagoner, Editors, *Sea Level Changes—An Integrated Approach Soc. Econ. Paleontol. Mineral., Spec. Publ.* **42**, 125-154.

Posamentier, H.W. and Vail P.R. 1988, Eustatic controls on clastic deposition, II. Sequence and systems-tracts models. In: C.K. Wilgus, B.S. Hastings, C.G.St.C. Kendall, H.W. Posamentier, C.A. Ross and J.C. Van Wagoner, Editors, *Sea Level Changes—An Integrated Approach Soc. Econ. Paleontol. Mineral., Spec. Publ.* **42**, 125–154.

Posamentier, H.W. and Allen, G.P., 1993, Variability of the sequence stratigraphic model: effects of local basin factors, *Sediment. Geol*., 86, 91-109.

Postma, G., Kleinhans, M.G., Meijer, P.Th. and Eggenhuisen, J.T., 2008, Sediment transport in analogue flume models compared with real-world sedimentary systems: a new look at scaling evolution of sedimentary systems in a flume. *Sedimentology*, 55, 1541–1557.

Postma, G., 2001, Physical climate signatures in shallow- and deep-water deltas. *Global and Planetary Change*, 28, 93-106.

Prins, M.A., Postma, G., Cleveringa, J., Cramp, A., Kenyon, N.H., 2000, Controls on terrigenous sediment supply to the Arabian Sea during the late Quaternary: the Indus Fan. *Marine Geology,* 169, 327-349.

Rahaman, W., Singh, S. K., Sinha, R., and Tandon S.K., 2009, Climate control on erosion distribution over the Himalaya during the past ~100 ka, *Geology* 37, 559-562

Ruddiman W. F., *Earth's climate; Past and Future*, 2001, 4th printing W.H freeman and Co. USA

Rossignol-Strick, M. 1983, African monsoon, an immediate climate response to orbital insolation. *Nature* 304, 46–49

Schlager, W., 1993, Accommodation and supply - a dual control on stratigraphic sequences, *Sedimentary Geology*, 86, 111-136.

Schumm, S.A. & Lichty, R.W., 1965, Time, space, and causality in geomorphology, Am. J. Sci., 263, 110-119.

Sømme, T.O, Helland-Hansen, W., and Granjeon, W., 2009, Impact of eustatic amplitude variations on shelf morphology, sediment dispersal, and sequence stratigraphic interpretation: Icehouse versus greenhouse systems, *Geology*, 37, 587-590

Steel, R., Mellere, D., Plink-Björklund, P., Crabaugh, J., Deibert, J., Loeseth, T. and Shellpeper, M., 2000. Deltas v rivers on the shelf-edge: their relative contributions to the growth of shelf-margins and basin-floor fans (Barremian and Eocene, Spitsbergen). In: *GCSSEPM Foundation 20th Annual Research Conference Special Publication, CD*, GCSSEPM, pp. 981–1009

Tuenter, E., Weber, S. L., Hilgen, F. J., Lourens, L. J., 2003, The response of the African summer monsoon to remote and local forcing due to precession and obliquity, *Global and Planetary Change*, 36, 4, 219-235

Vail, P. R., Mitchum, R. M., Jr., Todd, R.G., Widmier, J.M., Thompson, S.,III, Sangree, J.B., Bubb, J.N., and Hatlelid, W.g., 1977 Seismic stratigraphy and global changes of sea level, In Clayton C.E.., editor, *Seismic stratigraphy - Applications to hydrocarbon exploration; American Association of Petroleum Geologists Memoir* 26, 49-212

Van Heijst, M.W.I.M., and Postma, G,. 2001, Fluvial response to sea level changes: A quantitative analogue experimental approach, *Basin research*, 13, 269-292.

Van den Berg van Saparoea, A.-P., and Postma, G., 2008, Control of climate change on the yield of river systems, In: Hampson, G.J., Steel, R.J., Burgess, P.M., and Dalrymple, R.W., eds., *Recent advances in models of siliciclastic shallow-marine stratigraphy, Volume Special Publication* 90, Society of Sedimentary Geology.

Van der Zwan, C.J., 2002, The impact of Milancovich-scale climate forcing on sediment supply, *Sedimentary Geology,* 147, 217-294

Woodruff, F., and Savin, S.M., 1989, Miocene deepwater oceanography, *Paleoceanography, 4*, 87-140.